NON-DESTRUCTIVE EVALUATION OF CORRODED AND CORROSION REPAIRED RC BEAMS

A Dissertation Submitted
In Partial Fulfillment of the Requirements
for the degree of

MASTERS OF ENGINEERING
IN
STRUCTURAL ENGINEERING

Submitted by:
Sunil Garhwal
(ROLL NO. 801422026)

UNDER THE SUPERVISION OF
DR. Shruti Sharma
Associate Professor
Civil Engineering Department
Thapar University, Patiala

DEPARTMENT OF CIVIL ENGINEERING
THAPAR UNIVERSITY,
PATIALA-147004
JULY 2016

DECLARATION

I, Sunil Garhwal, hereby declare that this thesis entitled **"NON-DESTRUCTIVE EVALUATION OF CORRODED AND CORROSION REPAIRED RC BEAMS"** in fulfillment of the requirement for the award of the Degree of **Master of Engineering** in **Structural Engineering** and submitted in the Civil Engineering Department, Thapar University, Patiala is an authentic record of my work carried out during a period from July 2015 to July 2016 under the supervision of **Dr. Shruti Sharma, Associate Professor** Department of Civil Engineering, Thapar University, Patiala.

This matter presented in this thesis has not been submitted by me for the award of any other degree of this or any other University.

Date: 14/07/2016

Sunil Garhwal
Roll No. :801422026

CERTIFICATE

This is to certify that above statement made by the student concerned is correct and true to the best of my knowledge and belief.

26/7/2016

Dr. Shruti Sharma
Associate Professor
Department of Civil Engineering
Thapar University, Patiala- 147004

Countersigned by

Dr. Naveen Kwatra
Professor & Head
Department of Civil Engineering
Thapar University, Patiala-147004

Dr. S.S.BHATIA
Dean of Academic Affairs
Thapar University, Patiala-147004

i

ABSTRACT

Reinforced concrete structures have suffered the deterioration due to corrosion despite the protection that concrete provides to embedded steel. Since steel corrosion remains unnoticed inside the concrete, it further accelerates and can cause loss of life and property. This report discusses the effects of deterioration caused to reinforced beams due to corrosion at different levels. six RC beams (127 x 227 x 4100) mm were cast one was kept as control beam and rest five of which were corroded to different levels i.e. (20days, 30days, 40days, 50days and 60days) by impressed current technique, while one remain as control beam . All five beams were subjected to vibration based health monitoring at the end of their respective corrosion period. This was done to investigate the effect of corrosion on dynamic properties of beams with increasing corrosion. Vibration characteristices of beams showed decrease in vibration amplitude and frequency of beam with increasing level of corrosion. After dynamic analysis ,each beam was tested under static two-point loading and corresponding loads and deflections were recorded along with Acoustic emission hit parameters were recorded which showed the behaviour of crack. The static load deflection characteristices of beams corroded to different level shows decrease in load carrying capacity, deflection capacity with the increase in age of corrosion. Most importantly it was noticed that as corrosion increased the failure mode of beams shifts from predictable ductile failure to brittle failure.

ACKNOWLEDGEMENT

The success of any project requires a lot of guidance and assistance from many people and I am fortunate enough to have it all along the completion of my work. Constant inspiration and encouragement given by all was the driving force that kept me going throughout this project.

To begin with, firstly I would like to thank Almighty for giving me the strength to complete this thesis peacefully and successfully.

I express my sincere thanks and gratitude to my Respected Supervisor Dr. Shruti Sharma, Associate Professor, Department of Civil Engineering whose valuable guidance and continuous support helped me keep my morale high during my work.

I am grateful to Dr. Naveen Kwatra, Head of Civil Engineering Department, for giving me the opportunity to do this project. I also owe my sincere thanks to the other teachers of both the department for their all time guidance and assistance.

I owe my profound gratitude to the non-teaching staff of the department of civil engineering for their consistent cooperation and help throughout the thesis work.

This endeavour of mine would not have been possible without constant support and encouragement from my parents and my friends. I would like to show my sincere gratitude to my beloved friends for making this time so cherishable and standing with me during the tough times.

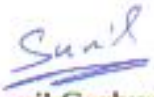

Sunil Garhwal

CONTENT

LIST OF FIGURES

LIST OF TABLES

CHAPTER 1

INTRODUCTION

1.1 BACKGROUND AND MOTIVATION

One of the most serious concerns in civil structures are damage and deterioration of reinforced concrete. Corrosion is one of the most serious type of deterioration. Deterioration because of corrosion is a matter of concern in countries like India because of exposure of structures to adverse environmental attacks caused due to long coast lines, severe monsoon and acid rain. The estimation of corrosion and effective measures to restore the structures is important to ensure the safety of structures. For performing conventional repair method included removal of concrete is done from the delaminated area and then the affected steel is cleaned and covered with cement mortar. But these measures were not enough to stop corrosion. Other methods frequently used for preventing corrosion are application of corrosion inhibitors, cathodic protection and extraction of chlorides.

The load carrying capacity of the structure is affected invariably by the corrosion. Thus, along with corrosion inhibition for restoring the structures, increasing its strength is essential. Out of all strengthening techniques the most popular one is FRP bonded to the external faces of damaged RC structures. This provides better durability, handling and improved mechanical properties over the conventional methods. When FRP sheets are bonded to RC members there is negligible increase in the dimension or weight of the sheets. Their ease of application, high durability in adverse environments and high strength to weight ratio makes them the most preferred material of repair.

1.2AIMS AND OBJECTIVES

The objective of this study is to monitor the damage in a RC beam due to corrosion of reinforced using various non-destructive methods these include

- Study of deterioration due to corrosion in RC beams using global vibration technique and local AE technique.

- Along with non-destructive technique destructive test were also carried out in the form of study of flexural behaviour of the beam under two point loading
- Further the non-destructive technique and destructive testing was also extended to repair corrosion affected beams using GFRP.

1.3 CORROSION IN REINFORCED CONCRETE

In reinforced concrete structures the corrosion of steel occurs which is one of the major obstacles and economic issues faced by concrete industry. It is a threat to the durability of structures. Due to widespread use of RC structures, this problem is so common and has become unavoidable. Normally, the reinforcement (steel) is unaffected by corrosion as concrete ordinarily provides high alkaline environment. Because of the high alkalinity, a thin invisible protective passive film of ferric oxide (Fe_2O_3) is formed. It is expected that when a thick covering of low permeability concrete is use to protect an embedded steel from the air, the corrosion of steel would not arise. But this expectation is not fully met in practice and this is evident from the damage caused in RC structures due to corrosion of steel.

There are two stages in corrosion with rusting in reinforcement of concrete. First stage includes the aggressive elements, like carbon dioxide and chloride (CO_2) (Cl^-), present in the surrounding environment which penetrates in the concrete. This is a primary stage, it involves the transfer of aggressive agents (mainly carbon oxide and water) of water and oxygen, including the corrosion initiation (depassivation of reinforcement). The secondary stage involves the propagation which starts, when these aggregates bodies are in rather high concentrations at the reinforcement's level. This agrees to the rust growth, which leads to the formation of cracks and could break the concrete cover. In this stage occurs growth of corrosion, leading to concrete damage, spalling and cracking of the concrete cover (**Figure 1.1**), etc. This stage starts when the contents of aggressive agents are high enough close to reinforcing steel.

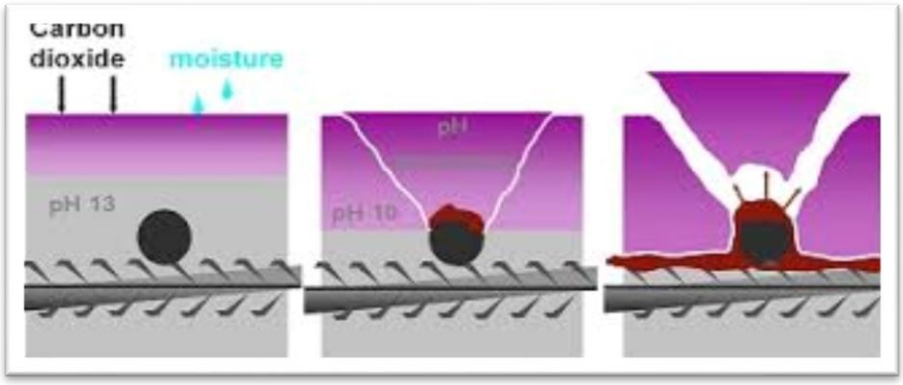

Figure 1.1: Cracking and spalling of concrete cover due to corrosion of reinforcement [1]

Finally, the lubricant effect of corrosion products and cracking of concrete cover cause bond deterioration at steel-concrete interface which reduces the load carrying capacity and service life of RC structures resulting in a severe damage [*2*]. **Figure 1.2** shows the effects of steel corrosion on concrete structures.

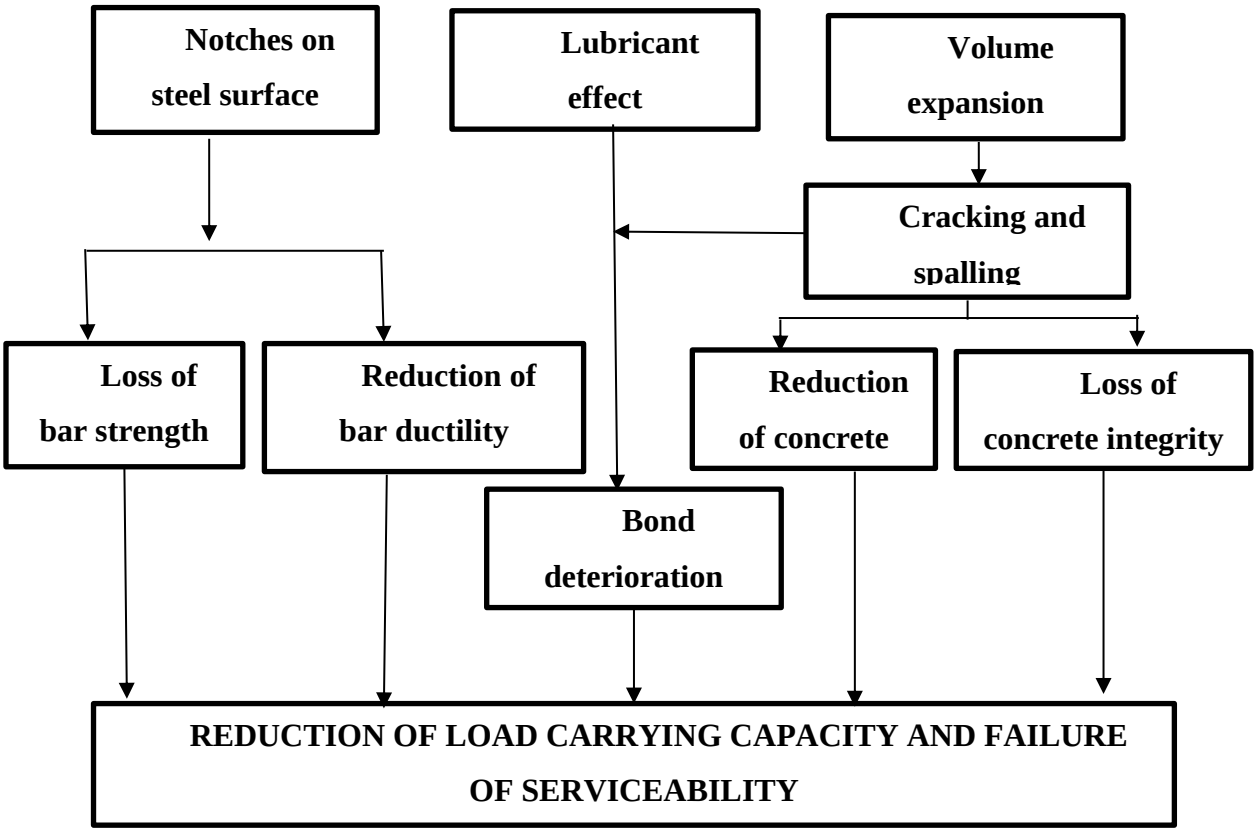

Figure 1.2 Effect of steel corrosion on concrete structures [*2*]

1.3.1 Causes of Rebar Corrosion

The corrosion behaviour of reinforced steel in concrete is determined by the composition of pore solution of concrete and chemical properties of steel. The concrete parameters other than pore solution composition, also affect rebar corrosion. The environmental factors do not directly affect steel corrosion, but cause damage to concrete cover and accelerate the ingress of aggressive species, making pore solution in contact with concrete more corrosive. Among all the environmental factors, the two most important factors responsible for corrosion of steel in concrete structures are the chloride ions and carbon dioxide. The various factors that are responsible for rebar corrosion are due to the presence of:

1. **Chlorides:** the chloride is present in concrete in two forms :
    - Free chloride, dissolved in pore solution.
    - Bound chloride, absorbed on cement gel or combined with hydrated cement and aggregates.
2. **Carbon Dioxide**
3. **Moisture**
4. **Type of steel**
5. **Pore solution of concrete**
6. **Permeability of concrete**
7. **Temperature**
8. **Thickness and defects of Cover Concrete**.
9. **Concrete Resistivity**

1.3.2 Corrosion Mechanism

The corrosion of reinforcing steel in concrete is an electrochemical process .An electrochemical process involves transfer of electrons form one material (anode) to the other (cathode). When no external electrical source is present, two half cell reactions occur, one at the anode and other at the cathode. The anode produces electrons resulting in the oxidation of iron (Fe) and the cathode consumes these electrons i.e. reduction of oxygen takes place to form hydroxyl ions (OH^-). These half-cell reactions take place in

the presence of an electrolyte. When these reactions occur close together, or at the same location, it is termed as microcell and when they take place at widely spread locations, it is termed as macrocell.

For any corrosion of metal, three basic processes take place which are as follows:

1. De passivation reagents, such as dissolved oxygen at the medium surrounding the surface of metal, or H^+ ion present in the aqueous medium arrive at the surface of metal.
2. Electrochemical reactions (i.e. oxidation and reduction reactions) take place at the interface between metal and the medium surrounding it.
3. Some corrosion products are formed on the surface of metal or removed from its surface to medium. For e.g., Fe^{2+} and OH^- ions move into the aqueous solution by anode and cathode respectively and, passive film or corrosion products are formed on the metal surface. The corrosion process can be stopped by the absence of any of the above process.

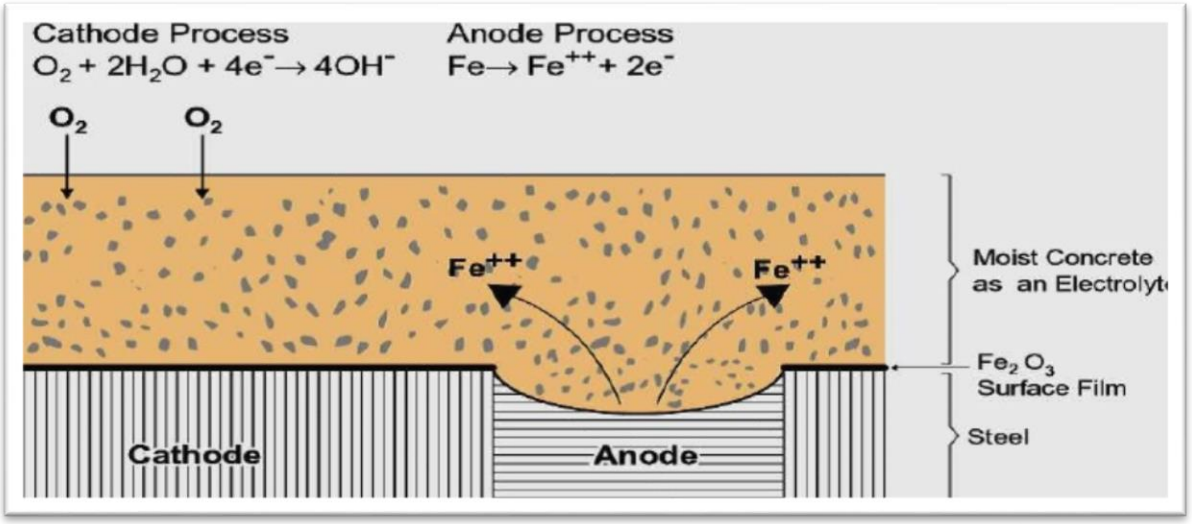

Figure 1.3: Corrosion Mechanism [3]

Corrosion of embedded steel in concrete is an electrochemical process. The surface of the corroding steel functions as a mixed electrode that is a composite of anodes and cathodes electrically connected through the body of steel itself, upon which coupled anodic and cathodic

reactions take place. Concrete pore water functions as an aqueous medium, i.e., a complex electrolyte. Therefore, a reinforcement corrosion cell is formed.

The electrochemical half - cell reactions taking place are:

At Anode:

$$Fe \rightarrow Fe^{2+} + 2e^{-}$$

$$2Fe^{2+} + 4OH^{-} \rightarrow 2Fe(OH)_2$$

$$2Fe(OH)_2 + \tfrac{1}{2} O_2 \rightarrow 2FeOOH + H_2O$$

$$Fe + OH^{-} + H_2O \rightarrow HFeO_2^{-} + H_2 \qquad \text{(2.1)}$$

At Cathode:

$$2H_2O + O_2 + 4e^{-} \rightarrow 4OH^{-}$$

$$2H^{+} + 2e^{-} \rightarrow H_2 \qquad \text{(2.2)}$$

The anodic reactions release intermediate corrosion product, Fe^{2+} into the solution continuously resulting in a loss of cross sectional area of steel bar. This may lead to external break down of the steel bar. Normally, the pH of pore solution ranges from 13 to 13.5 and only the first two anodic reactions take place. A protective passive layer is formed around the steel because of iron oxide Fe_3O_4 and Fe_2O_3. However, the ingress of chlorides and carbonates reduce the pH, depassivates the protective layer formed by oxides and initiates corrosion. Once the corrosion is initiated, it ultimately leads to delamination and cracking of concrete cover, thus exposing the reinforcement to the outside environment.

The various stages of corrosion are:

- Initiation
- Propagation
- Concrete Cracking

Initiation Stage describes the time period required for the occurrence of steel depassivation i.e., the time when aggressive species, such as chloride ions, carbon

dioxide, etc. penetrate through concrete to the surface of rebar (steel) and build up sufficient concentration of corrosion products to breakdown the passivation layer of steel. Propagation Stage describes the stage where active corrosion has already initiated. The corrosion rates at the propagation stage accelerate significantly once the concrete cover has cracked.

The increase in volume is responsible for concrete expansion and results in cracking, spalling and delamination in concrete structures.

1.4 Types of corrosion of steel in RC structures

Based on the corrosion mechanism and partly on the damage caused, corrosion of steel can be classified into following types:

- Uniform Corrosion
- Galvanic corrosion
- Localised Corrosion
- External current imposed corrosion
- Stress corrosion cracking and hydrogen induced constituent

The classification of corrosion types is not absolute but conditional.

1. **Uniform corrosion:** When the anodic and cathodic areas are very close to each other such that the distance between them is very small, then the electrochemical reactions would take place uniformly along the steel surface and the dissolution of steel occurs uniformly on the steel bar
2. **Galvanic corrosion :** Practically, the anodic and the cathodic reactions are not uniformly distributed on the steel surface and the rate of these reactions will vary .At some sites, anodic reactions may be faster while at other sites, cathodic reactions may be faster. Galvanic corrosion is dependent on the resistivity of concrete
3. **Localised Corrosion*:*** It is the most noticeable corrosion. It refers to the most dangerous corrosion damage to reinforcing steel. The various forms of localised corrosion are :
    - Pitting corrosion

- Crevice corrosion

The ratio of cathodic area to anodic area is very high resulting in an extremely high corrosion rate at anode. The significant feature of localised corrosion is that the corrosion is triggered and accelerated over a localised area, causing a decrease in pH and severe damage to the structure.

4. **External current induced corrosion:** This type of corrosion takes place when an external current is imposed on to a RC structure causing greater corrosion and a heavy loss of steel. Almost all the induced current is conducted by reinforcing steel because steel has greater conductivity than concrete.
5. **Stress Corrosion Cracking (SCC) and Hydrogen Induced Embrittlement (HIE):** SCC and HIE are found in some types of steel due to combination of particular corrosion media and stresses. They result in a sudden breakdown of reinforcement, thus leading to the collapse of RC structures. SCC and HIE are found in materials such as high strength steel. Though these types of corrosion are rarely found, the possible damage caused by them cannot be neglected [4].

1.5 CORROSION MONITORING IN RC STRUCTURES

This section gives an overview of the need of corrosion monitoring and various techniques by which it can be done.

1.5.1 Need of Corrosion Monitoring

It is assumed that reinforced concrete structures are durable because of their high tensile strength and high stiffness. However, this expectation is not met in practice and the failure of RC structures occurs when they are exposed to adverse environmental conditions over a period of time. This results in short service lives, high maintenance and repair costs. Hence, it becomes essential to monitor the development of corrosion problems in a new or existing RC structure prior to implementation of its repair or rehabilitation. Corrosion monitoring techniques are the corrosion measurement methods that give a complete picture of change in the condition of structure in time as well as in all three dimensions of the structure. The corrosion monitoring techniques give an

idea about the internal as well as external damage caused, thus enabling the engineer to provide suitable protection measures to the concrete structures.

1.5.2 Techniques used for monitoring of RC Structures

There are several methods for monitoring the corrosion of steel reinforcement in concrete. Corrosion monitoring gives a complete picture of the changing condition of a structure with time. In the last few decades, a number of techniques for damage detection such as Destructive and Non-Destructive techniques have been developed to analyse changes due to corrosion in structures.

1.5.3 Non-Destructive Testing Techniques

Non-destructive testing (NDT) is defined as the course of inspecting, testing, or evaluating materials, components or assemblies without destroying the serviceability of the part or system (Workman & O. Moore, 2012). The purpose of NDT is to determine the quality and integrity of materials, components or assemblies without affecting the ability to perform their intended functions. Non-destructiveness ought not to be confused with non-invasiveness. Testing methods that do not affect the future usefulness of a part or system are considered to be non-destructive even if they consist of invasive actions. The various non-destructive techniques to monitor corrosion in reinforced concrete structures are given below:

- Visual Inspection
- Infrared thermograph
- Electrochemical measurements
- Open Circuit Potential (OCP) measurements
- Surface Potential (SP) measurements
- Concrete Resistivity measurements
- Linear Polarisation Resistance (LPR) measurements
- Galvanostatic pulse transient method
- Electrochemical Impedence Spectroscopy (EIS)
- Cover thickness measure
- X-ray, Gamma Radiography measurement
- Vibration Measurements

- Ultrasonic wave
- Acoustic Emission

Most commonly used Non destructive techniques are :

Visual Inspection*:* This technique is based on structural analysis of the concrete surface with the help of binoculars or directly through eyes, once a month, an year or once in several years depending on the importance of structure. It uses visual information such as cracks, spalled concrete cover, rust stains, exposed reinforcement, etc. as a measure of corrosion monitoring. This method is not reliable as it is possible that corrosion has been initiated on reinforcing steel, but the symptoms on concrete surface are not visible yet. It might be too late when the symptoms are visible and the structure is severely damaged. Hence, this technique fails to detect corrosion at an early stage [5].

Concrete Resistivity Measurement*:* It is a NDT technique that evaluates corrosion risk on the reinforcement based on electrical resistivity measurements. The parameter "electrical resistivity" plays an important role in determining the intensity of corrosion. Greater the electrical resistivity of concrete material, slower will be the corrosion process. It has been reported that electrical resistivity is inversely proportional to the corrosion rate. Electrical resistivity is an important parameter that provides useful information about corrosion performance of steel embedded in concrete.

Linear Polarization Resistance (LPR) Measurements*:* It is a useful NDT technique that determines the instantaneous corrosion rate of reinforcing steel. This method provides more detailed information as compared to simple potential survey. Moreover, it is rapid, non-intrusive and enables accurate assessment of the condition of RC structures. However, this technique requires localised damage on the concrete cover in order to enable a concrete connection to the reinforcing steel. In this method, the potential of reinforcing steel is changed by a fixed amount ΔE and the current ΔI is monitored after a fixed time period. The change in potential ΔE should be between 10 – 30 mV (Stern-Geary range).

The polarization resistance, R_p is given as:

$$R_p = \Delta E / \Delta I \quad \_ \_ \_ \_ \_ \_ \_ \_ \_ \_ \_ \_ \_ \_ \_ \_ \_ \quad (2.3)$$

The corrosion rate, I_{corr} is expressed in terms of polarisation resistance (R_p)

$$I_{corr} = B/R_p \quad \text{(2.4)}$$

where, B is Stern–Geary constant.

B = 25 mV (for active steel)

B = 50 mV (for passive steel)

The value of corrosion current gives an indication of the condition of rebar.

In this study RC beams were subjected to different level of corrosion(that's 20 days, 30 days, 40 days, 50 days and 60 days) and corrosion monitoring is done using global vibration monitoring and local Acoustic Emission technique is used.

1.6 PROTECTION USING FRP's

This section provides an overview of common types of FRP materials used for providing passive and active protection against corrosion.

1.6.1 General

A number of researches have been done to find suitable composite materials that can be used for strengthening the newly constructed as well as old RC Structures. One such composite material that is in common use for the repair and rehabilitation of the structures is Fibre Reinforced Polymer (FRP). FRP delays the onset of corrosion on the reinforcement, thus extending the service life of the structures.

1.6.2 Suitability of FRP for use in Structural Engineering

Several factors have facilitated the use of FRP's for the repair and rehabilitation of RC Structures. Some of them are:

- Ease of installation
- High strength to weight ratio

- High durability
- Low permeability
- High thermal resistance
- Minimal architectural impact

FRP's can be laminated on the concrete surface using epoxy resin or can be used as inert anodes to delay corrosion of reinforcing steel in RC structures. When a structure is wrapped with FRP laminates, the corrosion activity is greatly reduced as FRP wraps act as a barrier to further penetration of water, oxygen and other aggressive species present in the environment. Moreover, FRP wraps provide an external pressure that resists the displacement caused by the expansion of corrosion products and reduce the cracking and spalling of concrete [2]. The FRP wrapped structures show an increase in axial compressive load capacity, improved flexural and shear load carrying capacity, increased ductility, increased torsional strength, increased fatigue resistance and an improvement of seismic performance [5]. FRP's are used as inert anodes instead of laminates, for the repair and maintenance of historical monuments and other heritage structures in order to preserve their physical appearance. Also, FRP protected structures are highly resistant to corrosive effect of salts, acids, alkalis under a wide range of temperature and are unaffected by the electrochemical and electromechanical deterioration.

1.6.3 Types of FRP's

Various FRP materials are available in the market out of which two materials are popular for providing protection against corrosion in India- glass and carbon.

(i) Glass Fibre Reinforced Polymer (GFRP): The GFRP covering act as a physical barrier that hinders the ingress of aggressive species such as chlorides and carbon dioxide present in the environment and strongly delays the corrosion onset. The properties of GFRP are shown in **Table 1.1** and **Figure 1.4** shows GFRP sheets.

Figure 1.4: GFRP sheet [7]

(ii) Carbon Fibre Reinforced Polymer (CFRP): CFRP sheets are thinner than GFRP sheets and exhibit a greater tensile strength, greater tensile modulus and lower ultimate strain. The properties of CFRP are shown in **Table 1.1**. **Figure 1.5** shows CFRP sheet.

Figure 1.5: CFRP sheet [8]

Table 1.1: Properties of CFRP and GFRP [6]

Material	Thickness (mm)	Tensile strength (GPa)	Tensile modulus (GPa)	Ultimate strain
Carbon sheet (Net fiber) (CS)	0.13	3.79	230	0.015
Glass sheet (Net fibre) (GS)	0.35	2.30	76	0.018
Adhesive	-	15	4.3	0.02

Maaddawy and Soudki (2005) investigated that CFRP repaired structures show greater flexural strengthening and a prolonged life as compared to unrepaired RC Structures, but significantly reduce the deflection capacity.

In this research work, Corrosion affected RC beams (20 days, 30 days, 40 days, 50 days and 60 days) under flexure and a RC beam repaired with GFRP, is monitored using global vibration monitoring technique and local AE technique.

1.7 CLOSING REMARKS

This chapter provided an overview of the theory of corrosion of reinforcement in RC structures and its propagation. Various corrosion monitoring techniques that are available for corrosion monitoring have also been discussed. For this study, Vibration monitoring technique has been chosen from all the available techniques for corrosion in RC beams and AE shall be used to monitor the flexural behaviour of corroded beams. Many methods that available for reinforcing the corroded RC beams are also discussed and it has been decided to use GFRP for retrofitting the RC beams.

1.8 FORMAT OF THESIS

The thesis has been divided into five chapters.

1st chapter is general introduction of corrosion in Reinforced concrete, types of corrosion of steel, its monitoring and utilization of FRP sheets for corrosion protection and FRP repair of structures.

2rd chapter Non-destructive techniques for corrosion evaluation

- Vibration monitoring technique
- Acoustic emission technique

3th chapter deals with the experimental program wherein all tests, procedures and measures to be followed during experiments are explained in detail.

4th chapter deals with the results and discussions where findings of the experimental program are explained in detail.

5th chapter is the concluding chapter.

CHAPTER 2

NON-DESTRUCTIVE TECHNIQUES FOR CORROSION EVALUATION

2.1 GENERAL

To inspect existing concrete structures, visual **i**nspection is the easiest and the most fundamental method. But this method may not be applicable for inspecting defects which does not appear on the surface of concrete. For such defects, Non-destructive inspection is the only method which can be applied there are various method which are adopted for non-destructive inspection. In this study, we shall be using NDT techniques which are:

- Global Vibration Monitoring Technique
- Local Acoustic Emission Technique

2.2 VIBRATION MONITORING TECHNIQUE

2.2.1 General

As the cracks initiation and propagation may occur at loads far below those for actual structural failure and, in the early stages it is possible to detect using visual inspection and other conventional means. However, vibration measurements are thought to be sufficiently sensitive to detect and monitor damage even when cracks are located well within a structure. A number of vibration based parameters have been used for structural health monitoring. The basic idea behind this technology is that modal parameters i.e. frequencies, mode shapes, and modal damping are the function of the physical properties of the structure which include mass, damping, and stiffness. Therefore change in the physical properties will cause detectable changes in the modal properties. Previous studies show that the modal shapes and damping can be used to detect damage.

2.2.2 Vibrational Signature

Vibration based structure health monitoring have been widely developed over the years to detect the damage in RC structures. Structural diagnosis by measuring and analyzing vibrational signals of any structure is a well-known method. If the new vibrational signature obtained during a routine operation deviates from baseline value than the structure should be checked for defects. This is called Vibration Signature technique. As damage normally associates with the stiffness of the structure, natural frequencies of structure will also change and hence these are the parameters most

commonly used for damage detection. The usual aim of vibration measurement is to predict response to given force or moment in different damage states[9];[12]. For stationary structures, the specific frequencies at which resonant amplitudes occur are called the natural frequencies of the structure, and these frequencies and the corresponding distribution of amplitude are global properties. The amplitude distributions at the natural frequencies and modes of vibration are known as the natural modes of vibration. Vibration responses of structures are related to structural weaknesses associated with resonance behavior, e.g., natural frequencies being excited by operational forces. It can be shown that the complete dynamic behavior of a structure in a given frequency range can be viewed as a set of individual modes of vibration. Each result has a characteristic natural frequency, damping, and mode shape. By using these so-called modal parameters to model the structure, problems such as specific resonances can be examined and subsequently solved. The first stage in modeling the dynamic behavior of a structure is to determine the modal parameters as introduced above:

(i) The resonant frequency or natural frequency

(ii) The structural damping

(iii) Frequency response functions

(iv) The mode shape

The modal parameters can be determined from a set of frequency response measurements between a reference point and a number of measurement points. Such a measurement point is usually called a degree of freedom (DOF). We record dynamic characteristics from OROS 8.0 NV gate solutions by striking the hammer just above the accelerometer. These dynamic characteristics include: Triggering, FRF records are explained below:

- **Triggering: -** Triggering is a technique for capturing an event for which it is not known exactly when it will occur. A trigger can start data acquisition and processing when a user specified voltage level is detected in and input channel. For example, we can set up a trigger to capture a hammer impact. After the trigger is armed, the analyzer will wait until the impact occurs before it starts acquiring data.
- **Frequency Response Function (FRF):-** FRF is computed from two signals. It is sometimes called a “transfer function”. The FRF describes the level of one signal relative to another signal. It is commonly used in modal analysis where the vibration response of the structure is measured relative to the force input of impact hammer or shaker. The

estimation of FRF depends upon the transformation of data from time to frequency domain. The Fourier transform is used for this computation. Unfortunately, though, the integral Fourier transform definition requires time histories from negative to positive infinity. Since this is not possible experimentally the computation is performed digitally using a Fast Fourier Transform (FFT) algorithm which is based upon only a limited time history. In this way the theoretical advantages of the Fourier transform can be implemented in a digital computation scheme.

- **Fast Fourier Transform (FFT):-** It is the discrete Fourier transform of a block of time signal. It represents the frequency spectrum of the time signal. It is a complex signal meaning that it has both magnitude and phase information.

2.2.3 REVIEW OF WORKS FOR VIBRATION MONIORING IN RC BEAMS

Salawu,(1997)**[10]** studied the use of natural frequency as a diagnostic parameter in structural assessment procedures using vibration monitoring is discussed in the paper. The approach is based on the fact that natural frequencies are sensitive indicators of structural integrity. Thus, an analysis of periodical frequency measurements can be used to monitor structural condition. Since frequency measurements can be cheaply acquired, the approach could provide an inexpensive structural assessment technique. The relationships between frequency changes and structural damage are discussed. Various methods proposed for detecting damage using natural frequencies are reviewed. Factors which could limit successful application of vibration monitoring to damage detection and structural assessment are also discussed.

Mirmiran and Philip (2000)**[11]** has conducted research in order to compare the acoustic emission signature of concrete beams reinforced with fiber reinforced polymer (FRP) or steel re-bars, a total of 16 203×203×1320-mm FRP-RC and steel-RC beams were tested under bending. The FRP-RC beams emitted higher activity and peak amplitude than their steel-RC counterparts. They also had lower felicity ratios, showed higher activity at each load drop, and emitted signals even during the unloading process. These characteristics were attributed to the lower stiffness, larger deflections, and brittleness of FRP re-bars, as well as their lower bond strength with concrete.

Burgueno et al. (2001)**[12]** Studied dynamic characterization of a full scale FRP composite bridge prototype of the Kings Storm Water Channel Bridge. Their research addressed the results of the modal vibration tests, and compared results as part of an assessment into its eventual use as a

standardized non-destructive health monitoring. They found that the modal vibration studies were a quick, effective, and relatively inexpensive, method for determining the dynamic structural properties. The modal vibration test data were successful in determining the changes in structural behavior due to changes in boundary conditions, as well as structural degradation or damage caused by loading.

Maia et al. (2002)**[13]** Present the subject of damage detection in structures. A series of numerical simulations on a simple beam are made in order to compare various damage detection methods based on mode shape changes. A generalization of these methods to the whole frequency ranges of measurement is proposed, i.e. methods based on mode shape changes become based on operational mode shapes. The objective of such a study is to ascertain the possibility of using various damage detection methods without the need for modal identification. He has developed some simple methods and tools based upon the use of FRF, which seem promising and have given good results in some practical applications. He also presented a new approach of FRF-based methods.

Kao (2003)**[14]** The proposed approach involved two steps. The first step, system identification, uses neural network to identify the undamaged and damaged states of a structural system. The second step, structural damage detection, uses neural networks to generate free vibration responses with the same initial condition or impulsive force. The inputs of the neural network are usually structural responses in time or frequency domain, or structural modal parameter (frequency, damping ratio, and mode shape), and the outputs are usually the damaged levels of members in the structure. He presented that change in structural properties (stiffness and damping) cause changes in periods and amplitudes of the free vibration of the structure system. Therefore, periods and amplitudes of the free vibration are useful indices to reflect changes of structural properties. The proposed approach makes it easy to accurately generate a free vibration response of an unknown structure system using neural networks.

Baghiee et al. (2009)**[9]**Studied the damage and CFRP strengthening of RC beams by vibration monitoring. They focused on the use of mode shapes and their derivatives. The Modal Assurance Criterion and Coordinate Modal Assurance Criterion factors were used to detect damage. These factors were derived from mode shapes and modal curvatures. They found that the modal assurance criterion was subjected to very small change by damage or strengthening. The coordinate modal assurance criterion factors might detect the changes in beam stiffness at degree of freedom.

Fan et al., (2011)**[15]** in this study on the damage identification methods are classified into four major categories: natural frequency-based methods, mode shape-based methods, curvature mode shape-based methods, and methods using both mode shapes and frequencies, and their merits and drawbacks are discussed. It is observed that most mode shape-based and curvature mode shape-based methods only focus on damage localization. In order to precisely locate the damage, the mode shape-based methods have to rely on optimization algorithms or signal processing techniques; while the curvature mode shape-based methods are in general a very effective type of damage localization algorithms. As an implementation, a comparative study of five extensively-used damage detection algorithms for beam-type structures is conducted to evaluate and demonstrate the validity and effectiveness of the signal processing algorithms. This brief review aims to help the readers in identifying starting points for research in vibration-based damage identification and structural health monitoring and guides researchers and practitioners in better implementing available damage identification algorithms and signal processing methods for beam- or plate-type structures

Capozucca, (2012)**[16]**Studied the occurrence of cracking damage in a structural, reinforced, concrete element leads to changes in its dynamic response. Nevertheless, the typical non-linear behavior of prestressed reinforced concrete (PRC) and reinforced concrete (RC) beams is characterized by cracking, due to the low tensile strength of concrete. It is necessary to take adequate account of cracking effects, in vibration-based monitoring of PRC/RC beams' structural health, by distinguishing cracking of tensile concrete due to bending moment under service loads; which does not reduce the structural availability of beams although it modifies their dynamic response, from real damage deriving from defects, loss of integrity and cracking due to overloading during service life.. This paper deals with cracking effects through an investigation of PRC/RC beam models in real scale, subjected to increasing static loading and natural vibration tests. Degradation of stiffness and development of cracking were related to frequency values measured in a frequency range through vibration tests on free end beams.

2.3 ACOUSTIC EMISSION TECHNIQUE

2.3.1General

Acoustic emission (A.E) is one of the most promising methods of monitoring of the structure at different stages of deterioration. AE technique can be adopted to forewarn the maintenance team

and to carryout repair work in a timely manner , thus saving the cost of repair and in prolonging the life of structures.Acoustic emissions are the waves that are generated as energy from elastic or plastic deformations occuring in the material . ASTM E 1316 (2006) defines acoustic emission as " the class of phenomena whereby transient elastic waves are generated by rapid release of energy from localized sources withun the material, or the transient elastic waves so generated ". AE waves can be generated as a result of various sources dislocations, microcracking and other changes due to increase in strain. The method is very senstive which enables it to detect damage long before its visible. AE sensors record the vibrations created by waves when they reach the materials surface. The peizoelectric crystal the detected wave to electric signal, amplify it(internally or using the external pre-amplifier), and send it to the data acquisition system. The passive ability of AE, external excitation or stimulus for data collection once sensors are placed, makes it a suitable candidate for real time monotoring and structural health monitoring of in-service structures. The method has also shown promise in assessment of damage during load tests of different structures and material including fibre reinforced polymer(FRP), steel, reinforced concrete(RC) and prestressed concrete(PC).

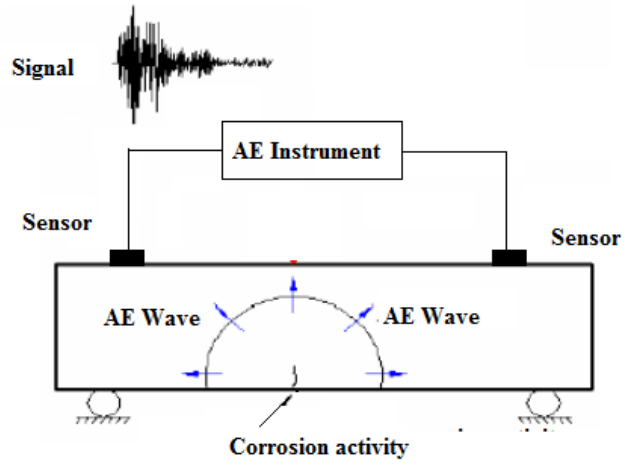

Figure 2.1: Schematic representation of AE Monitoring Process[17]

As indicated earlier, AE waves are generated from a sudden release of energy. The strength of AE signals depends on a number of factors such as distance and orientation of the source with respect to the sensor as well as nature of transferring material. Detected AE signals are usually referred to as hit. A more detailed analysis can be conducted on the waveform of each signal to calculate a number of parameters such as amplitude, rise time, duration, signal strength, energy, counts, etc. (ASTM E1316). The definitions of some commonly used AE parameters are described here:

- **Hit**
- Hit is the process of detection and measurement of an AE signal on an individual sensor cannel (ASTM E1316).
- **Event**

  Event is the rise of AE activity that will cause multiple hits on different sensors (ASTM E1316). A single event can be detected on multiple sensors.
- **Amplitude**

  Amplitude (also known as signal amplitude) is the largest voltage peak in the AE signal waveform; customarily expressed in decibels (dB) relative to 1 μV at the preamplifier input (dB) assuming a 40 dB pre-amplification. Decibels is the unit of measurement for AE signal amplitude A, defined by A (dB) = 20 log Vp; where Vp is the peak signal voltage in μV referred to the preamplifier input (ASTM E1316).
- **Duration**

  Duration is defined as the time from the first threshold crossing to the end of the last threshold crossing of the AE signal from the AE threshold (ASTM E1316).
- **Rise time**

  Rise time is the time from an AE signal‘s first threshold crossing to its peak (ASTM E1316).
- **Counts**

  Counts are the number of times the AE signal crosses the detection threshold (ASTM E1316).
- **Signal Strength**

  Signal strength is defined as he measured area of the rectified AE signal with units proportional to volt seconds (the proportionality constant is specified by the AE instrument manufacturer) (ASTM E1316).

$$\frac{1}{2}\int_{t1}^{t2} f_{+}(t)dt \quad + \frac{1}{2}\left|\int_{t1}^{t2} f_{-}(t)dt\right|$$

  where: is the signal strength, is the positive signal envelope function, is the negative signal envelope function, t1 is the time at first threshold crossing, and t2 is the time at last threshold crossing.

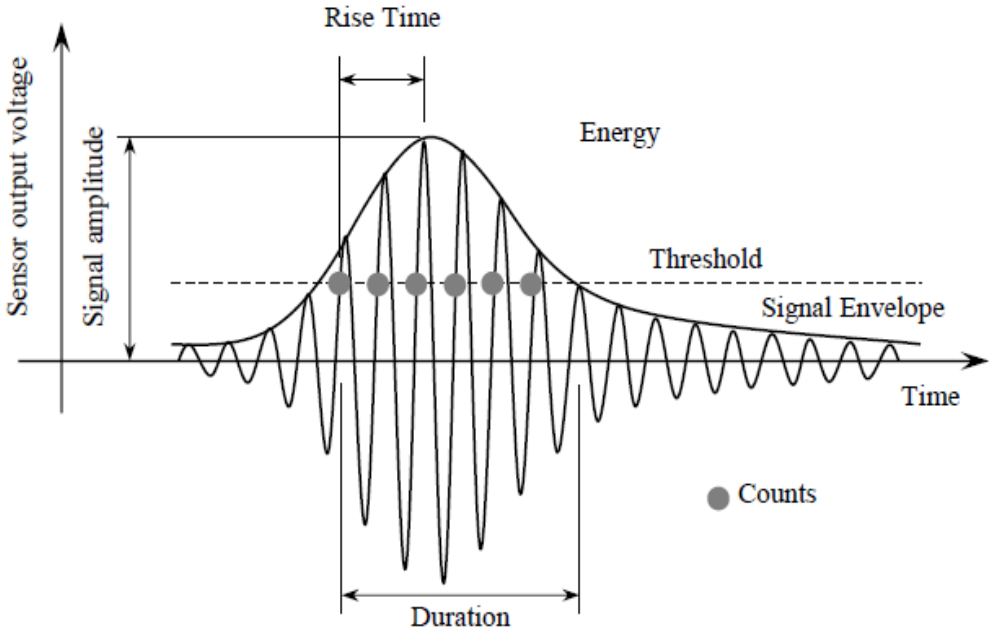

Figure 2.2: Schematic showing some parameters of an AE waveform [18]

- **Average Frequency**

  Average Frequency is the ratio between number of counts and the duration of the AE signal.

- **Peak Frequency**

  Peak frequency is the point in the power spectrum at which the peak magnitude occurs. The peak frequency is a 2 byte value reported in kHz.

- **RMS**

  The root mean square (*RMS*) is a measure of continuous varying AE voltage. It is defined as the rectified time averaged AE signal measured on a linear scale and reported in volts.

- **RA value**

  RA value is the ratio between rise time and maximum amplitude in Volts from an AE signal.

2.3.2 Acoustic emission source location

AE has the ability to locate the source of emitted waves. This technique is very similar to that used in seismology to locate the epicentre of earthquakes [19]. If the speed of AE wave in the tested material is known, source location can be performed using the arrival times of AE signals at

different sensor locations. Since it requires more than one sensor, only AE events are detectable using this technique. The algorithms that perform source location are well established and usually embedded in the data acquisition software. AE source locations can be done in a linear or planar or three-dimensional space based on the number of sensors used. AE source location is challenging since the nature of the material, presence of existing cracks in the source-to-sensor path, and the dimensions of the tested member might lead to false events as a result of wave reflections. Previous research showed that AE source location is feasible in RC or PC structures if proper filters were used [20].

2.3.3 Advantages of using acoustic emission technique

There are numerous advantages of using the Acoustic Emission Technique (**AE**) over the conventional NDT methods. Some of them are listed below:

- High sensitivity
- Early and rapid detection of defects, flaws, cracks etc.
- Real time monitoring
- Cost reduction especially maintenance cost.
- Defective area location
- It does not require access to whole area.

Hence, Acoustic Emission (**AE**) technique is a powerful aid to material testing and the study of deformation, fracture and corrosion. It gives an immediate indication of the response and behaviour of a material under stress intimately connected with strength, damage and failure.

2.3.4 Closing remarks

This chapter deals with corrosion mechanism in RC structures, factors affecting the corrosion process, need of corrosion monitoring in RC structures and various Non-destructive techniques used for corrosion monitoring in the structures. There is no denying from the fact that the NDT techniques can be used effectively for the investigation and evaluation of the actual condition of the structures. However, in this study we chose ultrasonic guided waves and acoustic emission technique for monitoring corrosion because of their advantages over other conventional NDT techniques. In the following chapter, work done by various researchers by using both these techniques will be discussed in detail.

2.3.5 REVIEW OF WORKS FOR ACOUSTIC EMISSION IN RC BEAMS

Weiss et al. (2000)**[21]** the acoustic emission (AE) behavior of reinforced concrete beam tested under flexural loading was investigated to characterize and identify different sources of damage including microcrack development, localized crack propagation, and debonding of the reinforcing steel. By testing plain, notched-plain, reinforced, and corroded-reinforced specimen, different damage mechanisms were isolated and characterized. AE events were analyzed using conventional AE parameters. In addition, waveform analysis was conducted using both fast fourier transform and wavelet transform method. The result of cross-plot, typically amplitude versus duration, showed a clean difference wih each stage of damage.

Colombo et al. (2005)**[22]** Study was conducted on alternative approach to the problem, based on "testing" the real structure rather than trying to model it. Experiments on reinforced concrete (RC) beams, representative of bridge beams, are described. The beams were loaded in cycles up to failure whilst recording the acoustic emissions (AE) generated. The analysis of the AE signals was then undertaken based on a proposed new parameter, named the "relaxation ratio". This quantifies the AE energy recorded during the unloading and loading phases of a cycle test and it showed a clear correlation with the bending failure load of the RC beams. A change in trend was noted when the load reached approximately the 45% of the ultimate bending load. The results appeared to be influenced by factors such as the concrete strength and loading rate and further work is needed to extend the results to full scale testing of bridge beams.

Yun et al. (2010)**[23]** In this study, the applicability of acoustic emission (AE) techniques to monitor damage evolution in reinforced concrete (RC) beams strengthened in flexure with carbon fiber reinforced polymer (CFRP) sheets is investigated. The parameters investigated in this study include both the amount of CFRP sheets and construction imperfections (the CFRP sheets were intentionally bonded without adhesive in the centermost 10% and 20% bonding area). The AE signals were collected and analyzed for all specimens. The AE parameters were analyzed for four levels of damage based on initial crack, propagation, yielding of main bars, and fracture or rip-off of the CFRP sheets. The frequency-peak magnitude distribution of the AE parameters was used to determine the *b*-value, defined by the Gutenberg–Richter relationship, for evaluating the damage evolution and fracture process of RC beams strengthened in flexure with CFRP sheets. From the results of this study, the signal characteristics – event, amplitude versus frequency, and amplitude versus duration – show clear differences in the different loading stages, depending upon the active

damage mechanism. The *b*-value is correlated to the fracture process of the RC beams bonded with CFRP sheets and the degree of localization of damage. The AE technique is a useful nondestructive technique for monitoring the behavior of RC beams that are externally reinforced in flexure with CFRP sheets.

Ohno and Ohtsu (2010)**[24]** study has been done on the fracture mode of cracking in concrete is normally changing from tensile mode to shear mode at impending failure. As for crack classification in concrete by acoustic emission (AE) techniques, two crack classification methods have been carried out. One of them is parameter-based method (parameter analysis) which has been carried out by employing two parameters of the average frequency and the RA value. The proportion of these two parameters, however, has not been determined yet. The other crack classification is simplified Green's functions for moment tensor analysis (SiGMA) procedure which is known as signal-based method. The SiGMA analysis is based on the generalized theory of AE, while the parameter analysis results from an empirical relation. Therefore, an optimal proportion of the parameter analysis is in great demand. In this study, these crack classification methods are compared and discussed from results of three types of concrete failure tests. As a result, ratios of the shear crack which are identified by SiGMA analysis are good agreement with those by parameter analysis in the case that the proportion of the RA value and the average frequency is set to 1–200.

Antonaci et al. (2012)[25] in this study an experimental analysis on two different sets of reinforced masonry walls under fatigue loading has been carried out. During these tests, the AE signals were recorded. The AE signals were analysed using Fast Fourier Transform (FFT) to examine the frequency distribution during the micro- and macro-cracking process. The evolution of the wavelength of the shear component of the AE signal was evaluated through the two characteristic peaks in the AE signals spectrum and the wave speed of the *P* or *S* waves. This wavelength evolution can provide information on the micro-crack and macro-crack progress. This procedure permits to estimate the characteristic fracture dimension in several loading conditions and for different masonry reinforcing methods.

Aldahdooh and Bunnori (2013)**[26]**study has been done on the application of the acoustic emission signal features in the structure health monitoring (SHM) fields. The most popular applications of acoustic emission signal in SHM are specified on crack monitoring, quantifying the degree of damage and crack classification. In this study, the acoustic emission signal is applied

to classify the types of cracks (flexural or shear cracks) of several types of RC beams subjected to four-point bending. Generally, the two common methods used in crack classification are the AE parameter analysis-based method and the signal-based method. The aim of this study is to classify the crack types of RC beams with varying thicknesses based on the fracture mechanism of the RC beams and the acoustic emission signal features. As a result, the ratio of shear cracks at the failure stage becomes 17.10%, 14.50% and 12.05% of the AE hits for the 20 cm, 25 cm and 30 cm beam thickness, respectively. These results coincided with the visual observation results according to crack modes. The results of the present application can be utilized in health monitoring of vital concrete structures such as bridges, and any RC member subjected to bending load. Which in term is used for prioritization of repair and retrofitting processes for these structures.

***Noorsuhada et al. (2013)*[27]** Fatigue crack classification on reinforced concrete beam is significantly vital. Acoustic emission (AE) signals were analysed to identify the classes of reinforced concrete (RC) beam corresponding to a specific crack mode. Third point loading fatigue test was carried out based on various range of maximum fatigue loading. The classification of crack for each phase of loading allowed the identification of the cracks mode of the beam namely tensile crack and shear crack. Average frequency and RA value were computed corresponding to channel basis and located event of AE signal and used to classify fatigue crack. The relationship between average frequency and RA value indicated clear trend with respect to crack classifications. Using this relationship trend, estimation of the crack monitoring can be made.

***Xiao et al. (2013)*[28]** In this study Acoustic emission (AE) acquiring technique was employed to explore the concrete fracture procedure in this study. Several parameters were evaluated through three-point bending beam tests using concrete fracture experiments. Acoustic emission instrument and strain gauges were used to monitor the initial and final fracture loads during crack propagation stage of specimens. In addition, the parameter values associated to crack propagations were obtained from the well-developed formula and test results. The typical trend curves and failure forms of each group of specimens were accompanied based on the crack-propagation theory. The designated concrete tests used in this study conducted a general process of crack fracture propagation. The experimental results indicated that AE detection system could well reflect the internal defects and cracks of the specimen. Additionally, the results illustrated that AE technology could reflect the initial fracture moment and final structure failure at a relatively low loading rate, and consequently could acquire the initial and failure fracture loadings. Based on this limited

study, it can be found that, in most cases, concrete AE parameter characteristic could reflect the concrete crack propagation and its complete structure failure during the loading procedure. Additionally, it was found that the test results from AE method were similar to those from strain gauge method

CHAPTER 3

EXPERIMENTAL PROGRAM

3.1 GENERAL

The objective of this study is to evaluate the efficiency of Non-destructive techniques (both global and local) for monitoring degradation encountered by large RC beams specimen undergoing anodic current corrosion. The global technique used is vibration diagnostic wherein change in frequency and amplitude of vibration signal will be recorded with progressive corrosion. Also, the destructive tests (load deflection tests) are conducted along with AE technique on order to evaluate the damage done by corrosion and the efficiency of GFRP in retrofitting corroded RC specimen.

3.2 TEST PROGRAM

The test program involved:

1. Determinations of basic properties of constituent materials namely cement, sand, coarse aggregate, steel bars as per relevant IS specifications.
2. Six real size RCC beams were caste of size (127 x 227 x 4100mm) using M20 desigining.
3. Five beams were corroded to different levels (20days, 30days, 40days, 50days and 60days) of corrosion using accelerated corrosion technique.
4. The beam corroded for 60 days at 10V constant voltage was repaired by GFRP (Glass fiber reinforced polymer) to improve its health.
5. Vibration signatures of all corroded and repaired beams were taken, to relate the effect of progressive corrosion with the dynamic characteristic of RC beams.
6. Effect of varying degree of corrosion on the load -deflection characteristics, all the six beams were also tested under flexural loading and simultaneously monitored using AE (Acoustic Emission)

The RC beam samples will be subjected to flexural test to determine load deflection characteristic. It will be further monitored using AE while undergoing flexural testing to evaluate the efficiency of NDT parameters with corrosion degradation. The corroded beams were repaired further with GFRP wraps and their health improvement was measured using both NDT and destructive parameters. **Figure 3.1** shows the complete test procedure in the form of flow chart

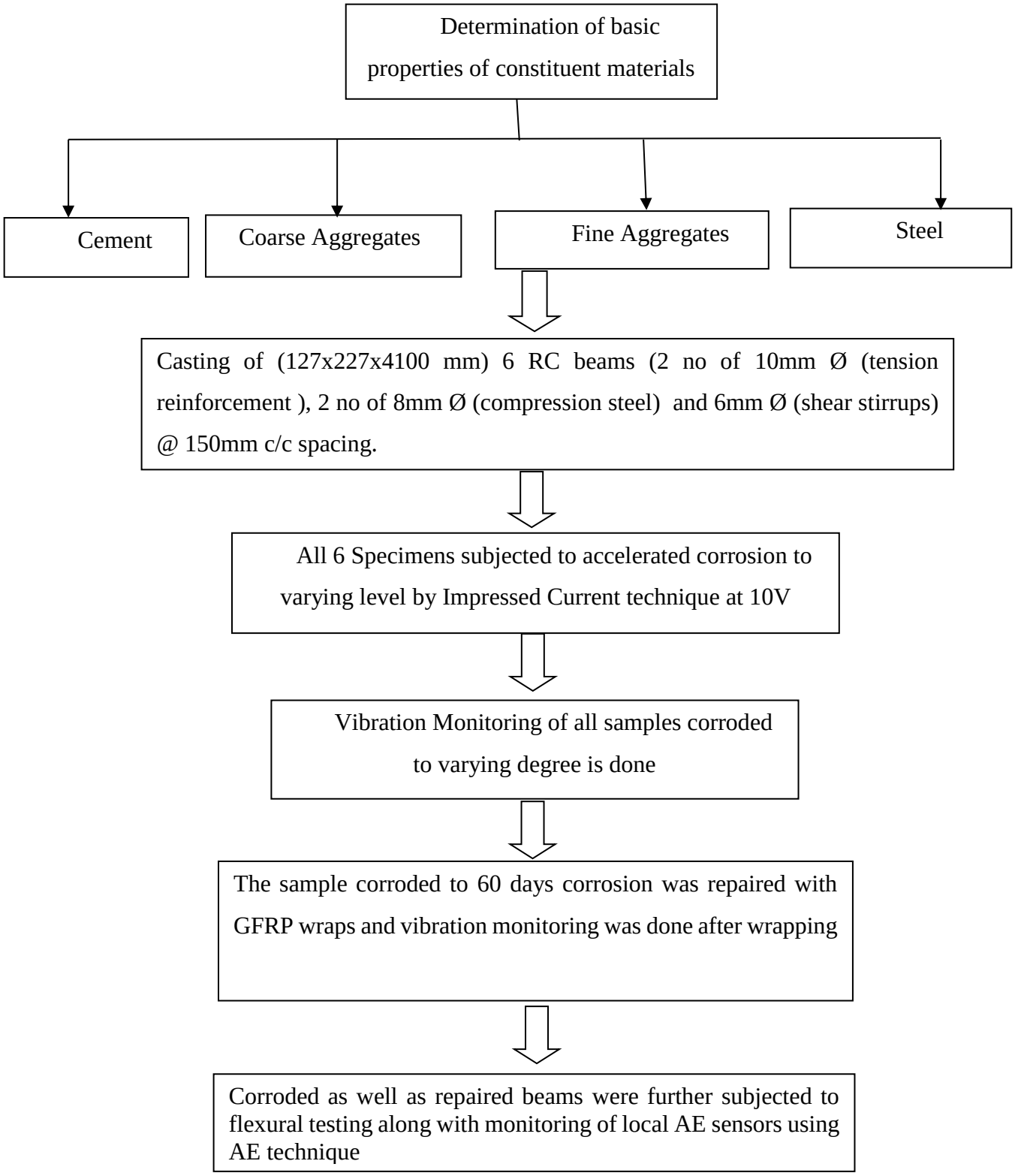

Figure 3.1: Flow chart of test program

3.3 MATERIALS USED

Cement, fine aggregates, coarse aggregates, water and MS bars are used in casting of slabs. The specifications and properties of these materials are as under:

- **Cement:** Ordinary Portland cement of 43 grade is used in study. The cement is of uniform colour i.e. grey with a light greenish shade and is free from any hard lumps. Summary of various tests conducted on cement are given in **Table 3.1**. All these tests are carried out in accordance with procedure laid down in IS: 8112-1989.
- **Fine aggregates:** The fine aggregates used for the experimental work is locally procured and conformed to grading zone III .Sieve analysis of the fine aggregate is carried out in the laboratory as per IS 383-1870.The sand is first sieved through 4.75 mm sieve to remove any particle greater than 4.75 mm sieve and then washed to remove the dust. The physical properties and sieve analysis of fine aggregates are shown in **Table 3.2** and **Table 3.3**.

Table 3.1: Physical properties of cement

S. No.	Characteristics	Experimented	Standard Values
1	Normal consistency	33%	_
2	Initial setting time	48 min	Not less than 30 min
3	Final setting time	240 min	Not more than 600 min
4	Fineness	4.8 %	_
5	Specific gravity	3.09	_
6	Compressive strength		

S. No.	Days	Experimental value
1	3	24.8 MPa
2	7	37.5 MPa
3	28	47.6 MPa

Table 3.2: Physical properties of fine aggregates

S. No	Characteristics	Experimental
1	Specific gravity	2.59
2	Bulk density	1.33 g/cm^3
3	Fineness modulus	2.63
4	Water absorption	0.89 %
5	Grading zone (based on percentage passing 0.60 mm) Zone III	_

Table 3.3: Sieve analysis of fine aggregates

Sr.No.	IS-Sieve (mm)	Wt. Retained (gm)	%age Retained	%age Passing	Cumulative % retained
1	4.75	14.5	1.45	98.55	1.45
2	2.36	37	3.70	94.85	5.15
3	1.18	246.5	24.65	70.20	29.80
4	600 µ	205.5	20.55	49.65	50.35
5	300 µ	287.5	28.75	20.90	79.10
6	150 µ	177	17.70	3.20	96.80
7	Pan	32	3.20		
	Total	**1000.00**		**SUM**	**262.65**

				FM =	*2.62*

Total weight taken of sample : 1000gm

Fineness modulus of fine aggregates = 2.68

- **Coarse aggregates:** Crushed stone aggregates (locally available) of nominal size 10 mm are used throughout the experimental study. The aggregates are washed to remove the dust and dirt and are dried to surface dry conditions. The aggregates are tested as per IS: 383-1970.The results of various tests conducted on coarse aggregates are given in **Table 3.4** and **Table 3.5** shows the sieve analysis results.

Table 3.4: Physical properties of coarse aggregates

S. No.	Characteristics	Value
1	Type	Crushed
2	Specific gravity	2.69
3	Water absorption	0.56 %
4	Fineness Modulus	6.91

Table 3.5: Sieve Analysis of Coarse aggregates

S. No.	Sieve size	Weight retained(gm)	Percentage retained	Percent Passing	Cumulative percentage retained
1	80	0.00	0.00	100.00	0.00
2	40	0.00	0.00	100.00	0.00
3	20	68.5	2.28	97.72	2.28
4	10	2776.5	92.55	5.17	94.83
5	4.75	113.5	3.78	1.38	98.62
6	Pan	0.00	0.00	0.00	
	Total	**3000.00**		**SUM**	**195.73 + 500 =**
				FM =	*6.95*

- **Water:** Fresh and clean tap water is used for casting slabs in the present study. The water is relatively free organic matter, silt, oil, sugar, chloride and acidic material as per Indian standard.
- **Steel reinforcement:** HYSD steel of grade Fe-415 of 10mm, 8mm and 6mm diameters were used as longitudinal steel. 10mm Ø bars are used as tension reinforcement and 8mm Ø bars are used as compression steel 6mm Ø bars are used as shear stirrups. The properties of these bars are shown in **Table 3.6**

Table 3.6: Properties of reinforcing bars used for casting specimens

Sr. No.	**Diameter of bars/ mesh wire**	**Yield-Strength (N/m2)**	**Ultimate strength**	**Percentage Elongation**
1.	10mm	440.55	513.2	15.1
2.	8mm	559.5	637.23	21.6
3.	6mm	449.2	612.8	32.5

- **Fibre Reinforced Polymer:** The FRP materials used for repairing are GFRP (Glass Fibre Reinforced Polymer) as shown in **Figure 3.2** :

Figure 3.2: GFRP laminate

The various properties of GFRP laminates as supplied by manufacturer are given in **Table 3.7**

Table 3.7: Properties of GFRP

Material	Thickness (mm)	Tensile Strength(MPa)	Tensile Modulus(GPa)	Ultimate strain	Electrical conductivity
GFRP	0.35	2.30	76	0.018	-

- **Adhesives:** The adhesive used for bonding FRP sheets with concrete is a compatible epoxy system (MBrace) as shown in **Figure 3.3**. It is blue pigmented resin for saturation of MBrace fibre sheet to form in-situ FRP composite. It is made by mixing base saturant and hardener in the ratio 100:40.Mixing of saturant and hardener is done thoroughly for five minutes until components are thoroughly dispersed. Properties of the epoxy are given in **Table 3.8**. as supplied by manufacturer.

Table 3.8: Properties of M brace saturant

S.No.	Properties	Values
1	Aspect	Translucent blue liquid
2	Density	1.13 ± 0.03 g/cm^3
3	Mixing ratio, by weight	100:40
4	Pot life	25 minutes at 25 degree
5	Tensile strength	> 17MPa
6	Compressive strength	> 40 MPa after 1 day
7	Flexural strength	> 35 MPa

Figure 3.3: Adhesive used for bonding FRP with concrete

3.4 DESIGN MIX PROPORTIONS OF CONCRETE

M20 grade concrete mix was used and prepared according to IS code method using the properties of materials as discussed above i.e. Table 4.1 to Table 4.6 The water-cement ratio was kept as **0.45**. The design mix proportion of the concrete were calculated as **1:1.425:2.7**(cement: sand: aggregate). Total six cubes of size (150 x 150) mm were cast for the compressive strength test. Three cubes were tested after 7 days of curing and rest 3 after 28 days. The average compressive strength of concrete after 7 days and 28 days comes out to be 16 and 28.5KN/m² which is within acceptable limits. **Table 3.9** shows Mix design proportion for concrete.

Table 3.9 Mix design proportions for concrete

	Cement (kg)	Sand (kg)	Aggregate (10mm)	W/C
M 20	1	1.425	2.7	0.45

3.5 RCC BEAM DESIGN

The beam used for experimental study is designed using limit state method (IS-4562000). It is designed as under-reinforced section. The beam is reinforced with 2 bars of 8 mm at compression

face and 2 bars of 10-mm at tension face 6mm stirrups were spaced at 150mmc/c Longitudinal section and cross-section of beam are shown in **Figure 3.4**

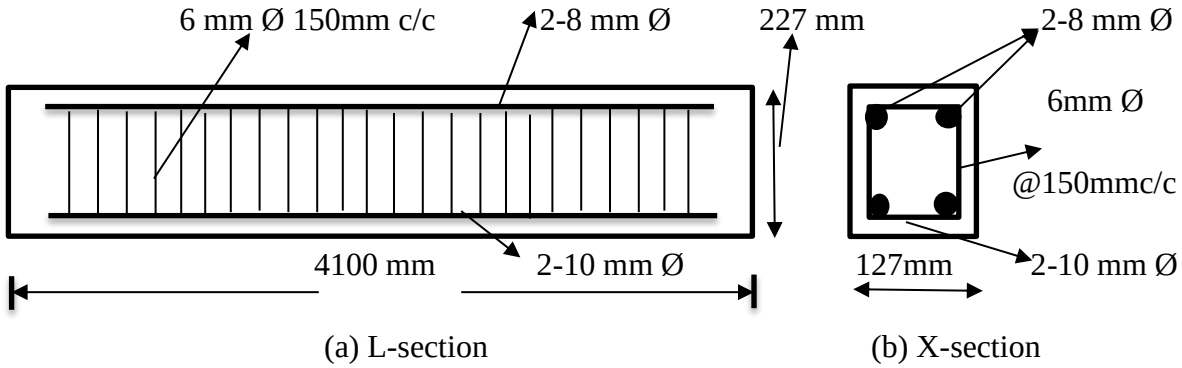

Figure 3.4 RC beam section detail used

3.6 CASTING OF COMPOSITE BEAMS

The casting of beams was done in single stage. The beams were cast in mould of size 127 x 227 x 4100 mm. Entire beam mould is first oiled so that the beam can be easily removed from the mould after 24 hours. Spacers of size 25mm are used to provide uniform cover to the reinforcement. When the bars have been placed in position as per design, concrete mix is poured in the mould and the beam is vibrated using a needle vibrator, to ensure the proper compaction. The vibration is done until the mould is completely filled and there is no gap left. The beams are then removed from the mould after 48 hours. After demoulding, the beams were cured for 28 days using jute bags.

Figure 3.5, Figure 3.6 and **Figure 3.7** shows the beams before and after casting.

Figure 3.5 Reinforcement detailing

Figure 3.6 Beam mould with reinforcement cage

Figure 3.7 Beam after casting

3.7 INDUCING CORROSION IN CONCRETE

The objective of inducing corrosion to the reinforcing bar is to simulate the corrosion damaged concrete. The commonly used methods of inducing corrosion in RC specimens can be recalled as Salt spray [28] , Chloride diffusion and impressed current method. Previous studies have shown that the test specimens kept in a salty spray chamber for more than 100 days did not show visible sign of corrosion. This method was not found suitable considering the time constraint. This method was not considered because it did not simulate the present condition of interest. Alternate immersion into NaCl solution and drying of the specimens also induces corro sion.

However, the quickest method of inducing corrosion is by impressing anodic current in this method, brine solution is supplied to the specimens and a direct current is passed making the reinforcement bar as an anode and another metal nobler than it in electrochemical series as cathode to induce corrosion.

Out of all six beams, five beams were corroded using impressed current technique for 20 days, 30 days, 40 days, 50 days and 60 days respectively. Initially one control beam was subjected to the accelerated corrosion until the longitudinal crack spread in the whole length of the beam, which took 60 days. And then the test matrix for the corrosion was further decided. So, rest two beams were subjected to 20 days, 30 days, 40 days and 50 days representing different levels of corrosion. The nomenclature of beams is given in **Table 3.10**

The corrosion of reinforcing steel was accelerated by impressed current technique. This was done through an integrated system incorporating a DC rectifier with a built- in ammeter to monitor the current and voltage to control the current intensity. Aplab Supply with a maximum output of 64V but the beams in our study were corroded at 10 V was used **Figure 3.8.** This method of corrosion was employed to reach advanced stages of deterioration in a relatively short time. At a time two beams were connected in series for corrosion process. Central 1.5 m portion of concrete beams were subjected to corrosive environment. It was done by continuous sprinkling of 3.5 % brine solution by water tank arrangement. This type of arrangement was selected to assure that the corrosion product formed is not washed away and cracks are formed in the concrete specimens. The direction of the current was adjusted so that the reinforcing steel became an anode and a

stainless steel wire mesh wrapped all around concrete beams at centre 1.5m served as a cathode. The tensile reinforcement(10mm Ø) was made anode and stainless steel wire mesh was made cathode (**Figure 3.10**)

Table 3.10 Nomenclature of beams

Beam	Corrosion level (in days)	Any detail
C-0	Corrosion for 0 days	-
C-20	Corrosion for 20 days	-
C-30	Corrosion for 30 days	-
C-40	Corrosion for 40 days	-
C-50	Corrosion for 50 days	-
C-60	Corrosion for 60 days	-
F-60	C-60 wrapped with GFRP	Wrapped after 60 days of corrosion

Figure 3.5 DC Regulated Dual Power Supply Source (constant voltage)

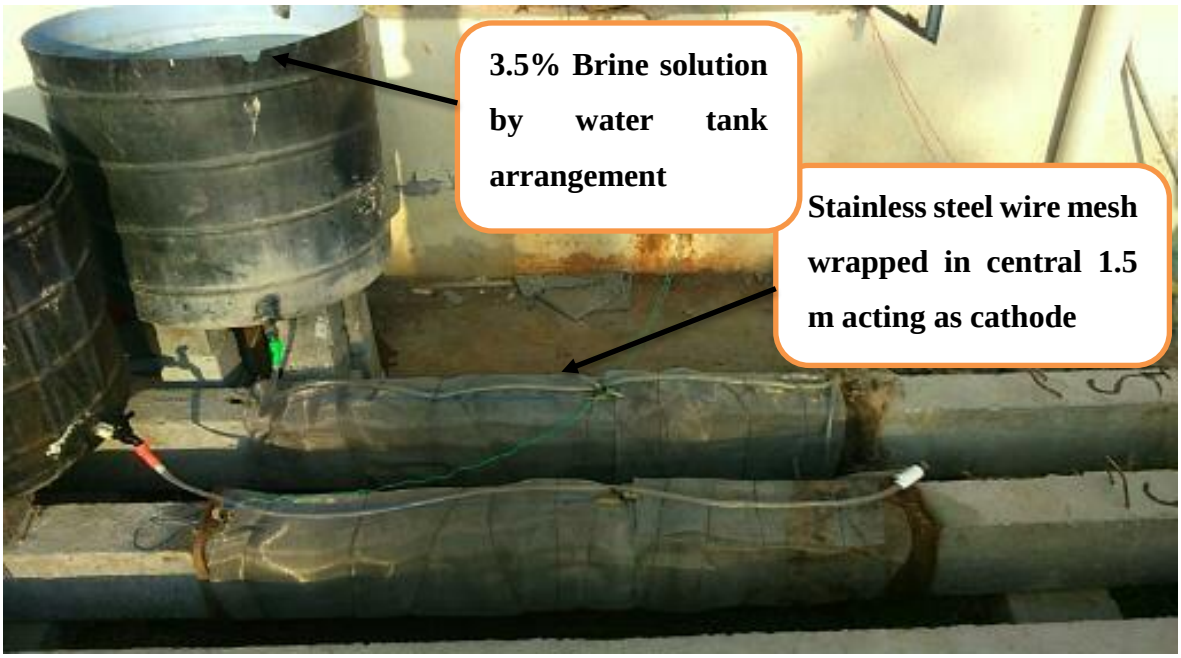

Figure 3.9 Stainless steel wire mesh wrapped around central 1.5 m part of Concrete beam served as cathode

3.8 REINFORCING THE CORRODED BEAM BY FRP WRAP

Two fibre materials are popular in the rehabilitation of structures in Indi a – Glass and Carbon fibres. The fibres are applied in the form of unidirectional sheets .Glass fibre sheets are thicker than the carbon fibre sheets. In this , commercially available, unidirectional GFRP sheets and compatible epoxy adhesive was used for repairing and retrofitting of corroded beams at 30 days and 60 days corrosion. The samples are air dried prior to the application of FRP wraps Manufacture's specifications are followed in the application of the wraps . A mixture of two component s of epoxy resin and hardener is mixed in the ratio of 100: 40 for wrapping the carbon fibre sheet into the carbon fibre sheets into concrete. Out of six specimens, two were wrapped with GFRP which were subjected to 30 days and 60 days of corrosion. . One layer of GFRP sheet was wrapped around the specimens with fibre along the length of the beam in middle 1.5m which was earlier subjected to acc. corrosion. A 25 mm overlap was provided at the ends of the sheets .

3.9 VIBRATION MONITORING

After all the beams subjected to different levels of corrosion, vibration characteristics of all beams were recorded using software OROS 8.0 using NV Gate solutions software. Vibration signatures were taken on C-0 and beam corroded to different level(C-20, C-30, C-40 and F-60). We recorded dynamic characteristics from FFT analyser by striking the hammer. The point for excitation were chosen as centre and one third of beam as shown in **Figure 3.10**

Figure 3.10Accelerometer placed below at centre and one third postion of beam

3.9.1 Equipment used in Vibration Monitoring

- **Accelerometer**

  Accelerations was measured at center and one third of the specimen using DYTRON model 11197 and 11305 with a sensitivity of 1.055 V/g. The accelerometer is shown in **Figure 3.11**. The data signal for each accelerometer was recorded at several sensitivity levels to allow reasonable resolution at all times over the exponentially decaying vibration signal. High strength cement plaster was used for mounting the accelerometer to the surface of the test specimen.

Figure 3.11 Accelerometers

- **Impact hammer**

The vibration response was measured by performing impact testing on the structure. An impact hammer having a hard rubber impact tip was swung from a horizontal distance of approximately 50 mm from the specimen [29]. The hammer was model PCB 20135 with a sensitivity of 0.00225V/N, made by OROS instruments. A typical impact-force hammer like the one used is illustrated in **Figure 3.12**. The impact consisted of a nearly constant force over a broad frequency range and was capable of exciting all resonances in that range.

Figure 3.6 Typical impulse-force hammer

- **FFT Analyzer**

  Spectrum analysis is defined as the transformation of a signal from a time-domain representation into a frequency-domain representation. There are four forms of the

Fourier Transform, explained as follows:

a) Fourier Series

b) Fourier Integral Transform

c) Discrete Fourier Transform (DFT)

d) Fast Fourier Transform (FFT)

the time domain signal obtained from vibration monitoring was subjected to FFT to get FRF (frequency response function). The NV gate did this transformation itself since it was an inbuilt function.

Figure 3.13: FFT Analyzer

3.10 STUDY OF LOAD DEFLECTION CHARACTERISTICS

After all the beams were corroded to different levels of corrosion and dynamic characteristics are studied, static load -deflection behavior of beam was studied to relate the effect of corrosion on RC beams. All the five beams (C-0,C-20,C-30,C-40,F-60) were tested under simply supported end conditions.

Ultimate load **P-Δ tests** were performed in the laboratory to determine the load carrying capacity of the beam specimens. The loading arrangement used was two-point loading. This arrangement allows for a central region having virtually constant moment without any shear force. Hydraulic operated jack in **Figure 3.14** and corresponding Data acquisition system in **Figure 3.15** is shown below:-

Figure 3.14 Hydraulic operated jack

Figure 3.15 Data aquisition system

The load is applied to the beam with the help of load cell and load value is obtained from the data acquisition system, which is attached with the load cell .One LVDT's is placed at the center of the beams to record the deflection against the loading as shown in **Figure 3.16**

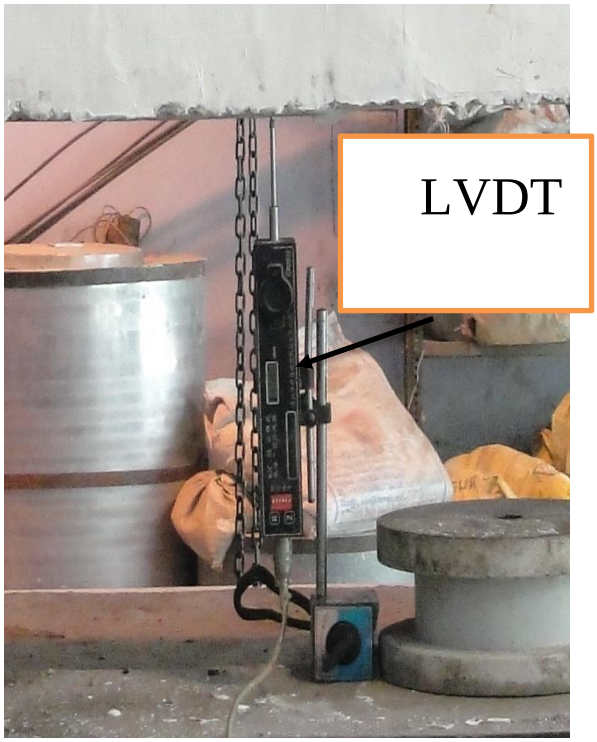

Figure 3.16 LVDT

3.11 ACOUSTIC EMISSION MONITORING

The phenomenon of acoustic emission is defined as the propagation of elastic waves due to release of localized internal energy, such as micro-fracture in elastic material. Structural deformation processes such as plastic deformation, crack expansion and other kinds of material degradation are the sources of the AE activity. Detection, amplification, filtering and analysing the signal are some of the important issues in AE technology. AE monitoring system typically consists of sensors, preamplifiers and AE acquisition and analysis system.In our study the corrosion process was accelerated by the impressed current technique. The research aims to identify the onset of corrosion by means of AE in RC specimens. The schematic representation of AE set up is as shown in the **Figure 3.17**:

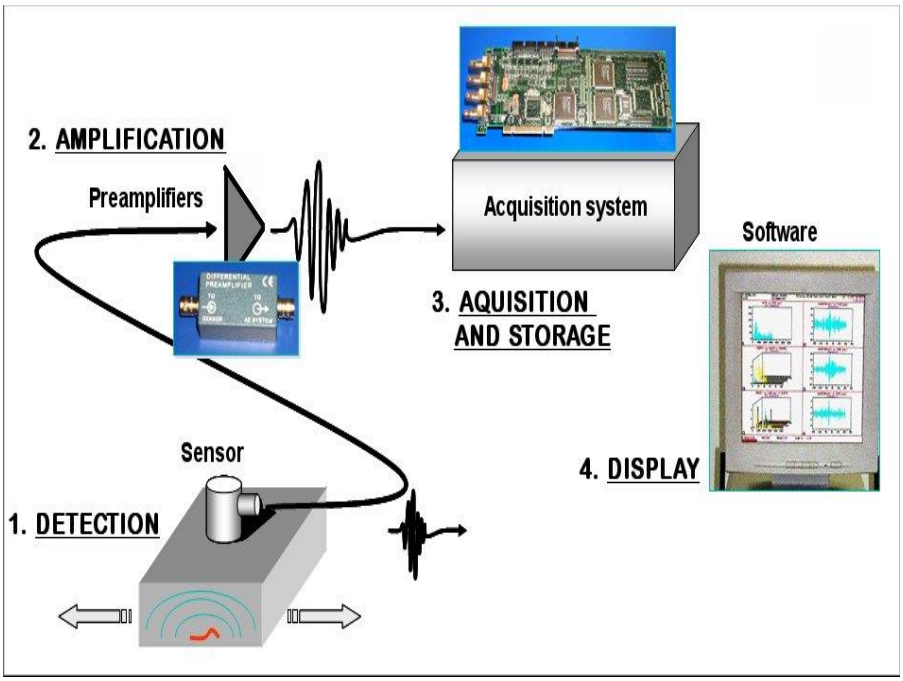

Figure 3.17 : Schematic representation of the AE monitoring

AE data acquisition system used for experimentation was Micro II digital AE system provided by PAC (Physical Acoustics Corporation) **MISTRAS GROUP** which is shown in the **Figure 3.18**.

Figure 3.18: Data acquisition set up used for the study

Sensors are placed on the surface of the structure to record acoustic emission signals. Sensors are available in wide range of shapes and sizes as shown in the **Figure 3.19**.

Figure 3.19: Acoustic Emission Sensors generally used

Acoustic Emission sensors which were used for monitoring the corrosion in the present study are shown in the **Figure 3.20**.

Figure 3.70: R3α Sensors for AE Acquisition used in the study

The specifications of the sensors used in the present study are shown in the **Table 3.11**.

Table3.11: Specifications of the sensors

Operating frequency range	35-100 KHz.
Resonant frequency	150 KHz
Physical Dimensions	19mm dia.× 22.4mm height
Weight	31 grams
Case Materials	Stainless Steel

Good coupling of the sensors to the test specimen is necessary for the effective transmission of AE signals. Sensors are attached on the surfaces using magnetic holders, glues, even rubber bands and tapes. A layer of couplant such as vacuum grease, ultrasonic gel, and oil is applied between the two surfaces. Operating frequency range is important during sensor selection. The common frequency range for AE testing in civil infrastructure is 100-300 kHz.

Experiment was carried out on a RC beam specimen of 127mmX227mmX4100mm along with a bar of 4400mm long and 10mm diameter embedded in concrete such that 150mm length is exposed to the environments from both sides. The acquisition system has 8 channels and is expandable up to 32 channels. However, we used six R3α sensors (resonant at 150 KHz) and preamplifiers with a gain set at 40 db and frequency range of 20-1200 KHz.

Two sensors were mounted on the front face of the RC beam specimen and two sensors were mounted on the bottom face of the beam specimen. The position of the sensors is shown in the **Figure 3.21**.

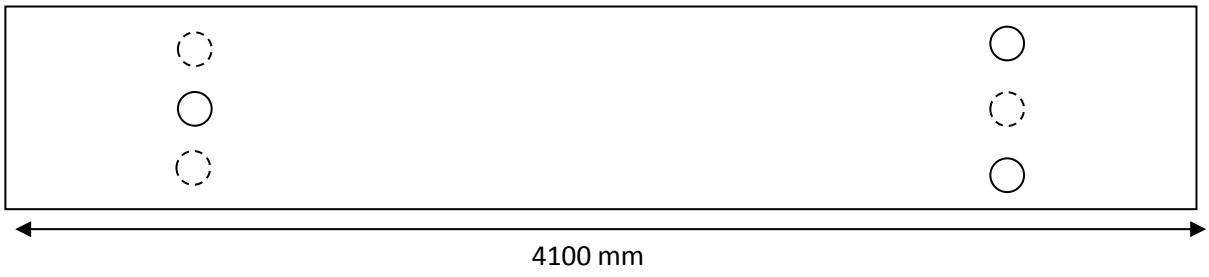

Figure 3.21: Location of sensors on the front face of the beam

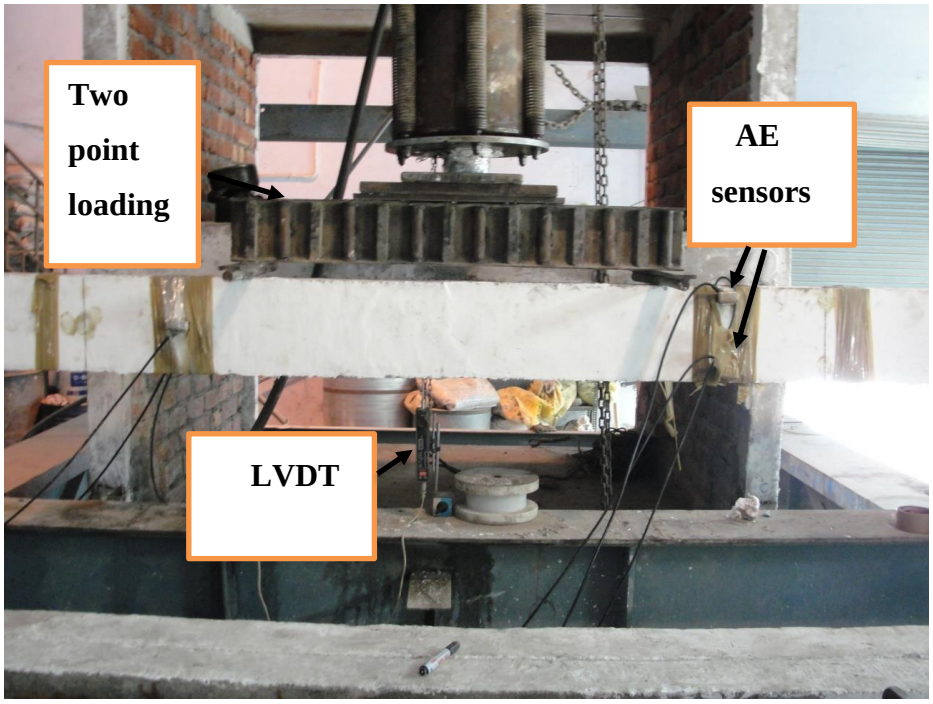

Figure 3.22: Actual sensors mounted on the beam

The AE signals were generated by breaking 0.5mm pencil leads on the selected locations on the surface of the RC beam specimen and in each position pencil lead break test were done twice. This was done to make sure that sensors are mounted properly on the RC beam specimen and they are able to detect the reflections though their amplitude would be smaller than the crack related signal. The AE process involves the use of sensors to detect released strain energy from the growing cracks. Hence, this technique has been widely used in the field of civil engineering for health monitoring.

3.12 CLOSING REMARKS

In this chapter methodology test matrix and experimental is discussed with details of basic testing of material used for casting RC beams, test and specimens details used for NDT and DT for monitoring progressive corrosion degradation in RC beams.

CHAPTER 4

RESULTS AND DISCUSSIONS

GENERAL

In this chapter, deterioration in RC beams subjected to varying degree of corrosion was studied by measuring the variation in crack pattern, effect on flexural load carrying capacity and deflections under static two point loading. Effect of same on dynamic characteristics of RC beams was also measured by using global vibration monitoring technique. The corroded beams while undergoing static loading were also monitoring using acoustic AE sensors attached to the beam to understand the crack propagation of corroded beams under loading. Also badly cracked corroded beam was repaired using FRP and its effect on destructive and non-destructive parameters were also measured.

4.1VISUAL INSPECTION

The visual inspection of a structure typically involves the search for large-scale deficiencies and deformities. As discussed earlier, initially one control beam was subjected to the accelerated corrosion until the longitudinal crack spread in the whole length of the beam, which took 60 days. And then the test matrix for the corrosion was further decided. So, rest four beams were subjected to 50days, 40 days, 30 days and 20 days of corrosion representing different levels of corrosion. So results of visual observation are discussed below in order of increasing corrosion level:-

4.1.1 Beam corroded to 20 days(C-20)

A beam undergoing accelerated corrosion for 20 days at a constant voltage supply of 10 V shows reddish brown patches of corrosion product on the three sides of beam at centre 1.5m portion of beam as shown in **Figure 4.1** It was noticed that no cracks were generated on surface of beam after 20 days corrosion. It was observed that at 20 days corroded beam shows small corrosion products with liquid oozey from the surface and no cracks as compared to badly corroded beams.

Figure 4.1 Red brownish products observed along the side

4.1.2 Beam corroded to 30 days (C-30)

Beam undergoing corrosion for 30 days at a constant voltage supply of 10 V shows reddish brown patches on three sides at centre 1.5m portion of the beam along with cracks on bottom and side faces. At the bottom of the C-30 beam flexural crack at centre with bending of beam was observed along with red brownish colored corrosion products as shown in **Figure 4.2**. At the front side face of the beam vertical cracks were observed originating from tension face towards compression face as shown in **Figure 4.3.** At the back side face of the beam it was observed that full centre 1.5m portion of the beam was covered with reddish brown patches, and longitudinal crack was observed on the surface throughout the centre 1.5m portion of the beam. A reddish brown liquid ooze out from the sides of beam is observed on both face of beam.

Figure 4.2 Cracks on left face of C-30

Figure 4.3 Longitudnal and tranverse cracks at right face of C-30

4.1.3 Beam corroded to 40 days(C-40)

Beams undergoing corrosion for 40 days shows dark reddish brown corrosion products with reddish brown liquid oozes out from the cracks on three faces of the beam at centre 1.5m portion. Corrosion products formed in C-40 beam was in large volume than in other cases. At the front side face longitudinal crack was observed throughout the centre 1.5m portion along the tension bar as shown in **Figure 4.4**.At the back face small vertical and horizontal cracks were observed with major vertical crack at centre. At the bottom face of beam large corrosion products were noticed and minor cracks were generated.

Figure 4.4 Longitudnal and tranverse cracks at right face of C-40

4.1.4 Beam corroded to 50 days(C-50)

Beams undergoing corrosion for 50 days shows dark reddish brown corrosion products with reddish brown liquid oozes out from the cracks on all three faces of the beam at centre 1.5m portion. Corrosion products formed in C-50 beam was in large volume than in other cases. At the front face of C-50 beam big vertical crack was observed throughout the centre1.5m portion of the beam as shown in **Figure 4.5** results into breaking of beam from the center part.

At the bottom face of beam large corrosion products were noticed but no major crack generated. It was noted that deterioration of C-50 beam due to corrosion was more than the other beams.

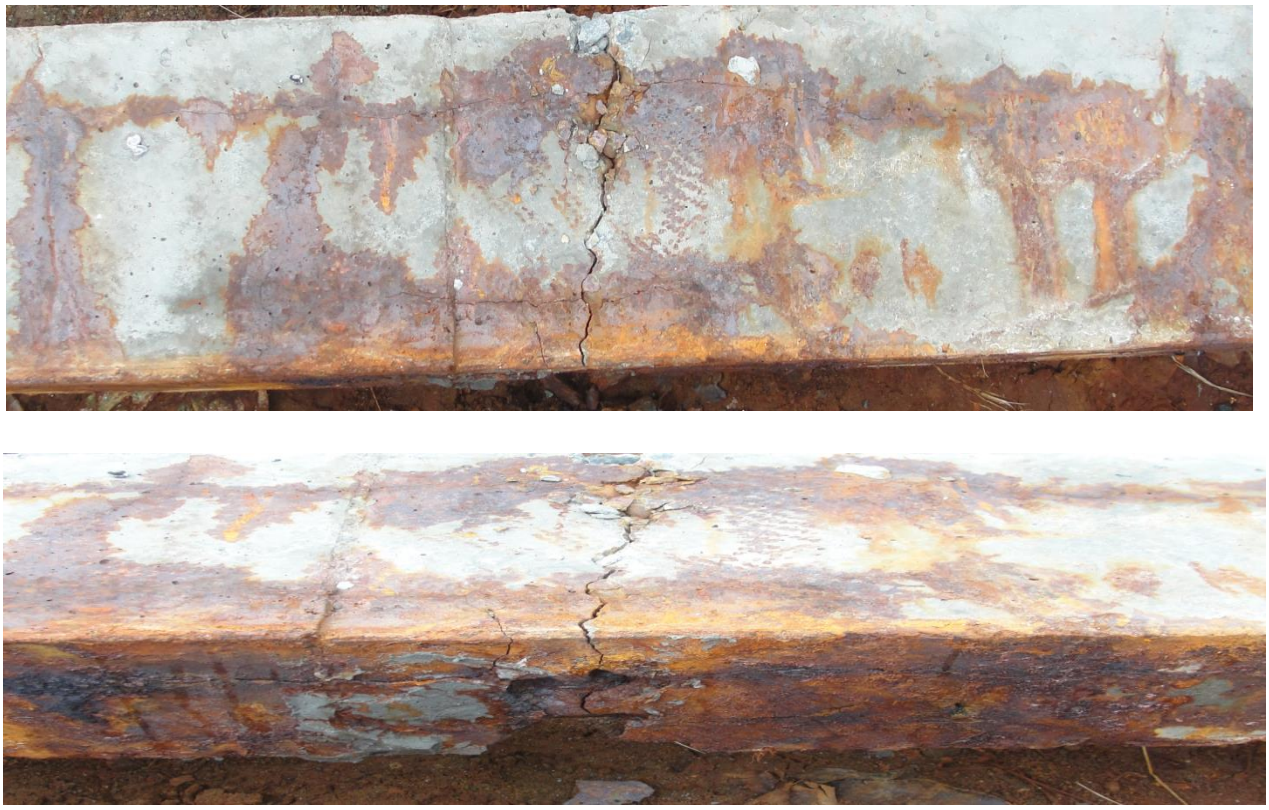

Figure 4.5 Right and bottom side of C-50

4.1.5 Beam corroded to 60 days(C-60)

Beams undergoing corrosion for 60 days shows dark reddish brown corrosion products with reddish brown liquid oozes out from the cracks on all three faces of the beam at centre 1.5m portion. Corrosion products formed in C-60 beam was in large volume than in other cases. There were horizontal cracks at the bottom face of the beam and large vertical and horizontal cracks were observed on both front and back side of beam. Thus to reinforce this sample it was wrapped with GFRP and further test were performed.

Figure 4.6 Right and bottom side of C-60

Figure 4.7 GFRP reinforced C-60 sample

4.2 VIBRATION CHARACTERISTICS OF RC BEAMS

In the experimental set up one beam is a control beam , one beam is reinforced by GFRP and other four beams are corroded beams at different levels i.e 20 days,30 days,40 days, 50 days and 60 days. The vibration characteristics were studied on control beam and corroded beam and results were compared. In this study, changes in structural dynamic characteristics of control beam and damaged beams were investigated using the OROS software program with the help of impact hammer excitation test. One accelerometer was installed at center of beams to measure the response. The program was set up to make a measurement with a frequency range of 0 to 50 Hz.

4.2.1 Control beam (C-0)

The fundamental frequency of control beam (C-0) comes out to be 18.5 Hertz and the FRF magnitude was 0.72 g/N as shown in **Figure 4.8**. Value of analytical frequency comes out to be 16.87 hertz. Error in experimental and analytical values of frequency comes out to be 9.67 %

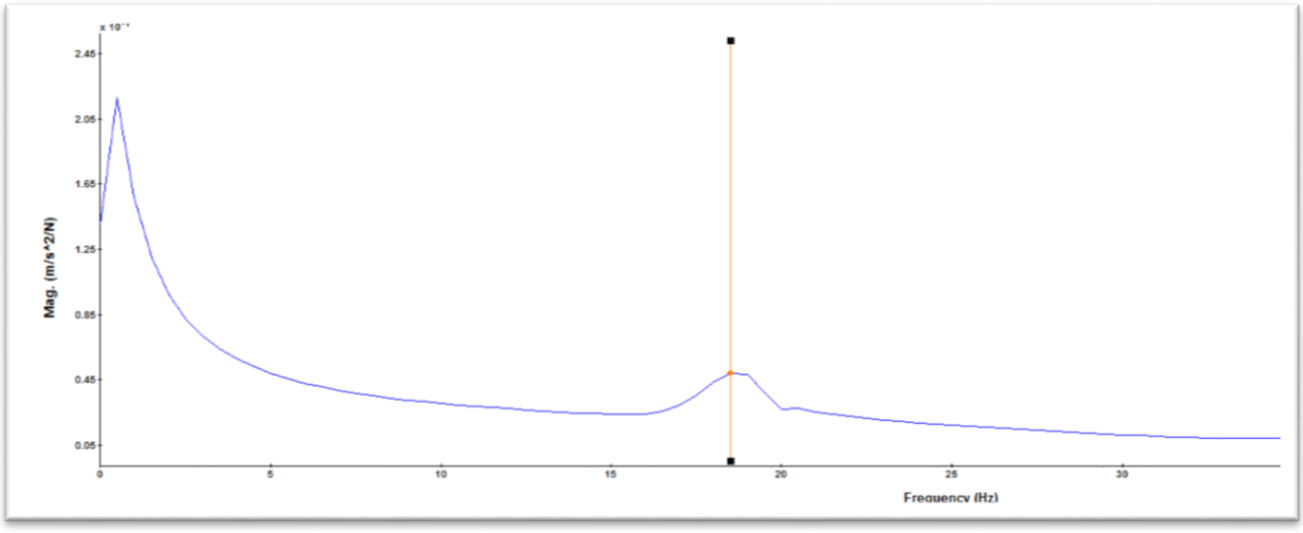

Figure 4.8 FRF record of C-0

4.2.2 Beam corroded to 20 days (C-20)

The fundamental frequency of corroded beam (C-20) comes out to be 16.5 Hertz and the FRF magnitude was 0.67 g/N as shown in **Figure 4.9.** As compared to control beam , frequency of corroded beam decreases from 18.5 to 16.5 Hz and so is the change in FRF magnitude, it also decreases as compared to control beam.

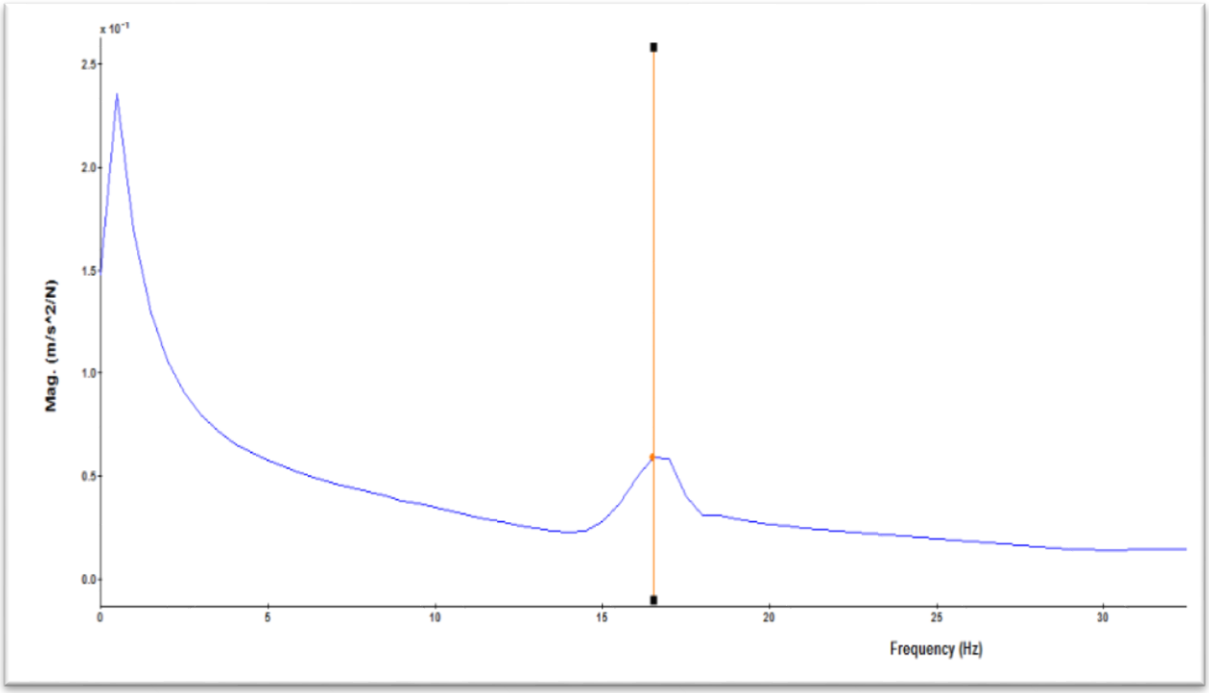

Figure 4.9 FRF record of C-20

4.2.3 Beam corroded to 30 days (C-30)

The fundamental frequency of corroded beam (C-30) comes out to be 16 Hertz and the FRF magnitude was 0.52 g/N as shown in **Figure 4.10.** As compared to control beam , frequency of corroded beam decreases from 16.5 to 16 Hz and so is the change in FRF magnitude, it also decreases as compared to control beam.

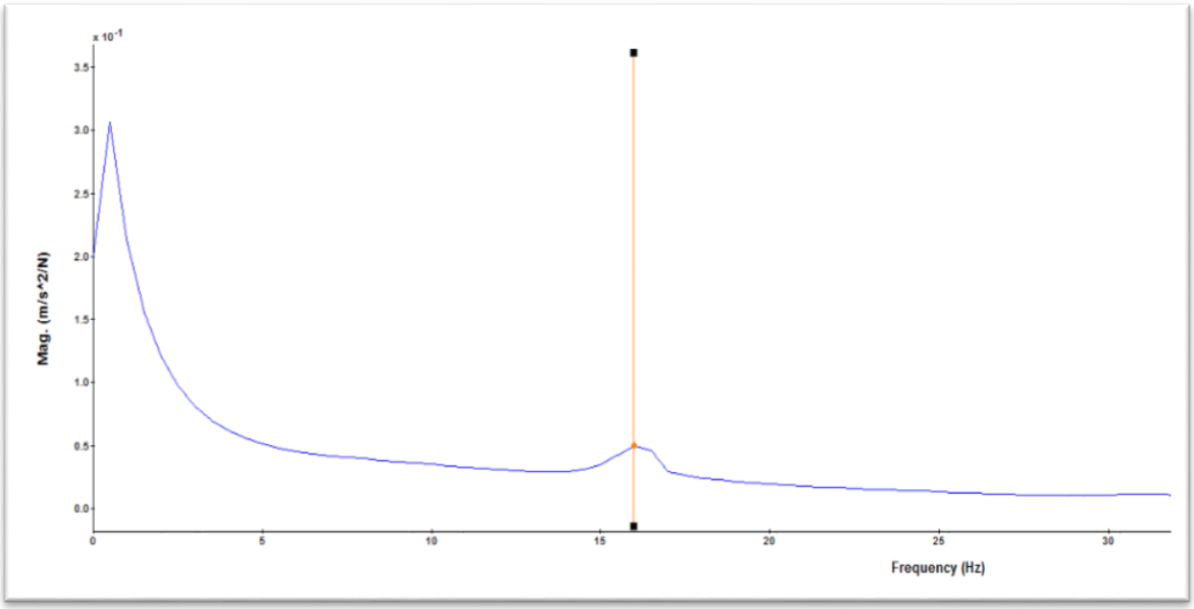

Figure 4.10 FRF record of C-30

4.2.4 Beam corroded to 40 days (C-40)

The fundamental frequency of corroded beam (C-40) comes out to be 16 Hertz and the FRF magnitude was 0.5 g/N as shown in **Figure 4.11**. As the corrosion level increases from 30 days to 40 days there is not much change in frequency but FRF magnitude slightly decreases as compared to beam corroded to 30 days, but if compared with corroded beam there is notable decrease in frequency and FRF amplitude.

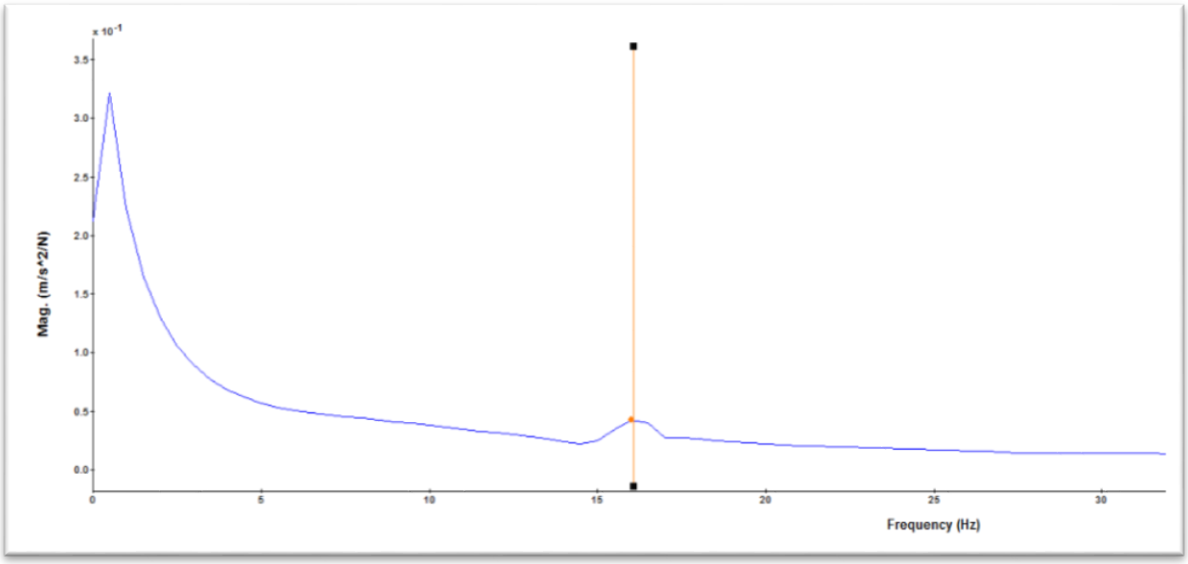

Figure 4.11 FRF record of C-40

4.2.5 Variation in frequency and FRF amplitude with different levels of corrosion

After studying the FRF records of all beams, minor shift in the frequency was observed as the level of corrosion increases.

- There is decrease in natural frequency with increase in corrosion. As the corrosion level increases in the beams ,cracks increases in beams results in decrease in frequency as compared to control beam
- It corroborates well with the increasing damage as observed in visual inspection with increase in corrosion.
- Similarly as the level of corrosion increases, load at failure reduces pointing towards stiffness loss with increase in corrosion
- In the same way as shown in **Table 4.1 and Figure 4.12** natural frequency falls due to huge degradation of beam due to corrosion. However at higher level of corrosion there is no significant decrease in frequency but its change in comparison of control beam is notable.

After studying the FRF records of all beams, drop in FRF amplitude was observed as the level of corrosion increases.

- FRF magnitude showed a huge decrease with increase in corrosion. As the corrosion level increases in the beams ,cracks increases in beams results in decrease in FRF magnitude as compared to control beam
- It corroborates well with the increasing damage as observed in visual inspection with increase in corrosion.
- In the same way as shown in **Table 4.1 and Figure 4.13** FRF amplitude decreases due to increasing degradation of beam because of corrosion

Table 4.1 Variation of frequency and FRF amplitude with level of corrosion

Sr. No	Beam	Fundamental Frequency (Hertz)	FRF amplitude (mg/N)
1.	C - 0	18.5	0.72
2.	C - 20	16.5	0.67
3.	C - 30	16	0.52
4.	C - 40	16	0.50

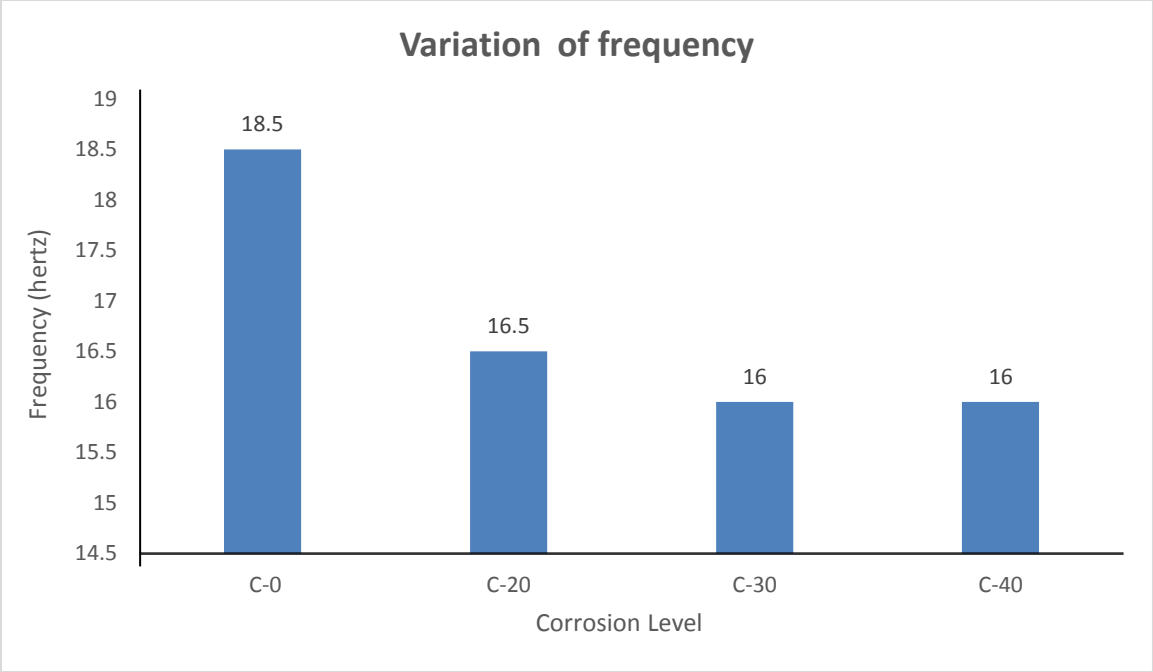

Figure 4.12 Bar chart showing relation between level of corrosion with frequency

Figure 4.12 shows graphically the variation of frequency with different levels of corrosion

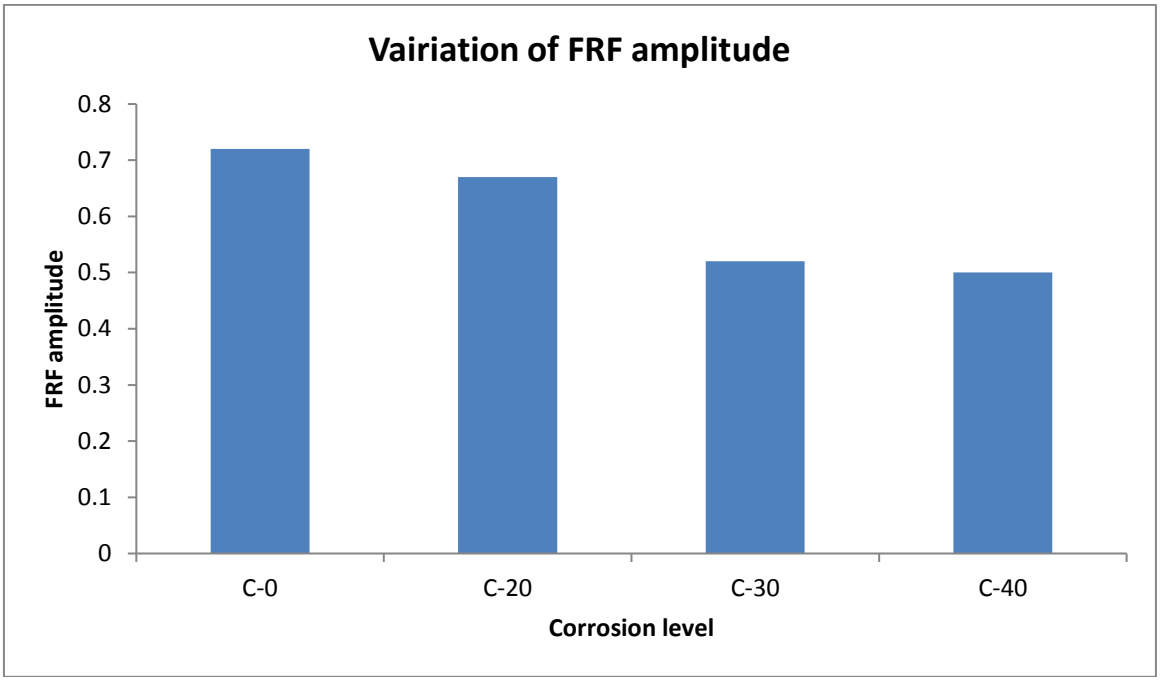

Figure 4.13 Bar chart showing relation between level of corrosion with FRF amplitude

From **Figure 4.13** it is clearly seen that as change in vibration charactersitics with increase in corrosion would not be a great indicator of corrosion degradation in flexural members through the

beam had reached degradation even after 40 days of acc. Corrosion. there is decrease in FRF amplitude as compared to control beam. From the recorded vibration characteristics of the corroding RC beams, it can be concluded that with global monitoring technique of vibration diagnostic only minor and normal shift and change in frequency and FRF respectively with degradation due to progressive corrosion as observed visually. It points towards use of a local corrosion monitoring technique would be more effective than global method.

4.3 LOAD DEFLECTION BEHAVIOUR OF RC BEAMS

After the corrosion process was completed, all beams including control beam tested for load deflection behaviour. Beams were loaded in two-point bending until failure and the corresponding load and deflections at midspan were measured using LVDTS.

4.3.1 Control Beam

The control beam (C-0) was tested under two point loading. The setup ensures pure bending in the central third portion of the beam. The beam was as shown in **Figure 4.14** and loads were applied till the failure and beam stop taking further load. It may be noted that the beam sections were under reinforced and steel yielded before concrete. The first crack appears at a load of 22.5KN near the left point load, accompanied by number of flexure cracks at the side face of control beam. As the load on the beam further increased the beam finally failed at 27.87KN. Almost all cracks were vertical near top and bottom edge, sub cracks were developed connecting to main cracks. So experimentally it was observed that ultimate load for the control beam is 27.87 KN with ultimate deflection at mid-span as 82.03mm.

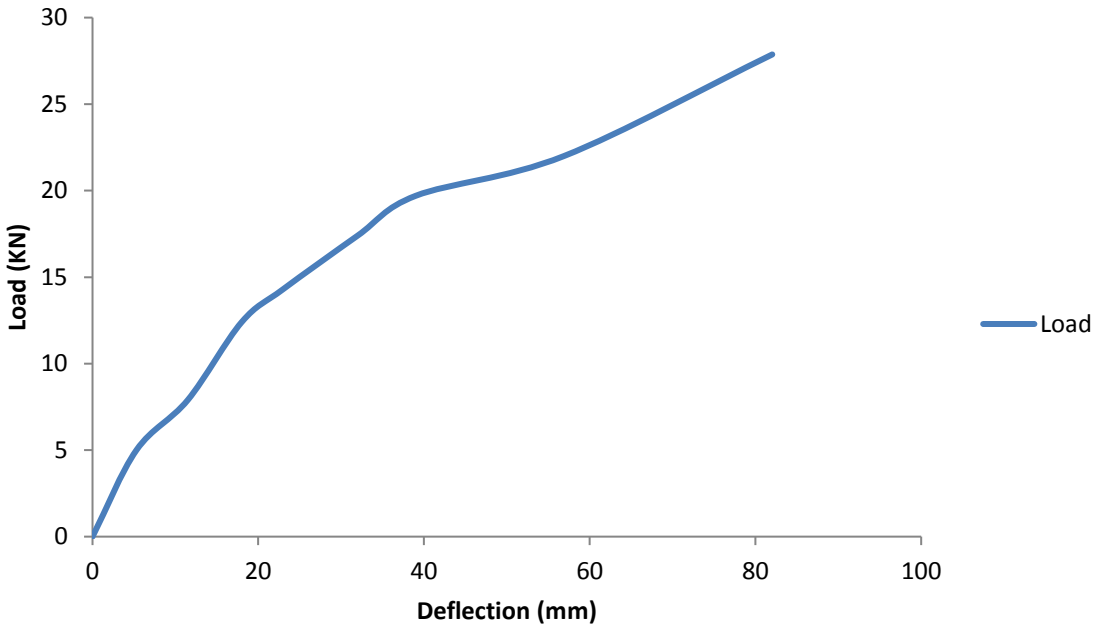

Figure 4.14 Load deflection curve of C-0 At L/2

Fig 4.15 Flexure Cracks on side face of C-0 beam

4.3.2 Beams corroded to 20 days (C-20)

Figure 4.16 shows beam with 20 days corrosion having no previous corrosion cracks as discussed earlier was tested under static loading. First crack appeared at a load of 18KN at centre of the beam near tension zone. Load is further increased the cracks widened and start progressing towards the compression zone and beam suddenly failed at load of 20 KN from extreme tensile face at centre as shown in **Figure 4.16**. No additional cracks appear on the surface of beam. P-Δ curves indicated

that there is a decrease in load carrying capacity and deflection capacity as compared to control beam. It was noticed from the results that there is decrease in load carrying capacity of C -20 beam as compared to control beam.

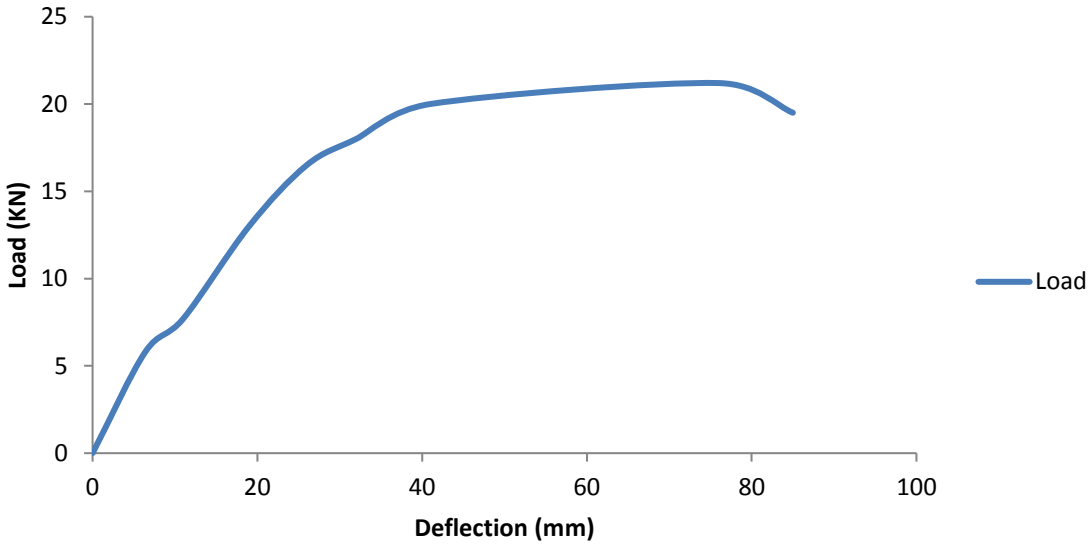

Figure 4.16 Load deflection curve of beam C-20 At L/2

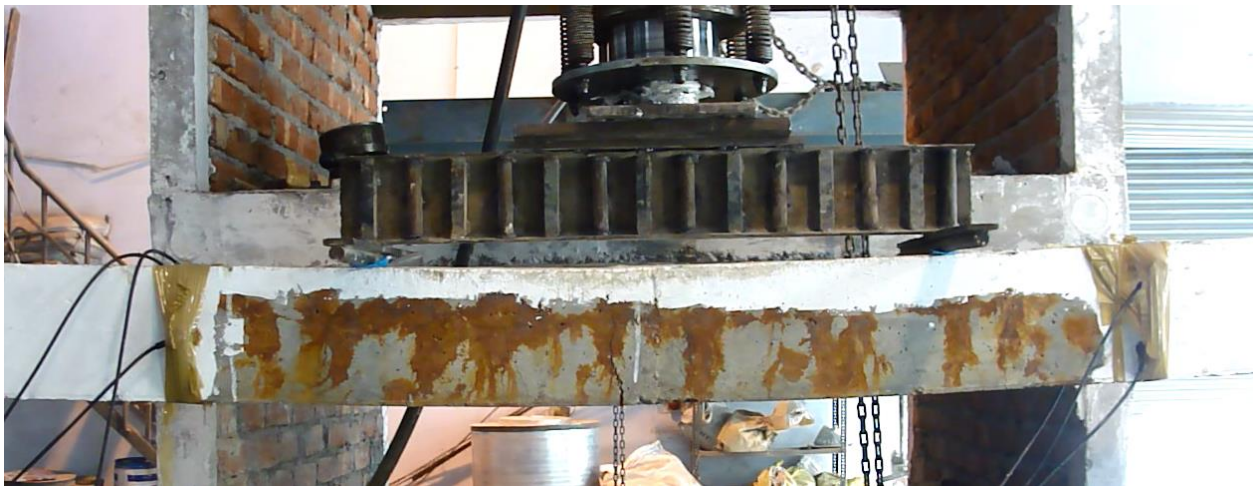

Figure 4.17 C-20 Beam showing large vertical crack near the centre of beam

4.3.3 Beams corroded to 30 days (C-30)

Beam undergoing corrosion for 30 days shows longitudinal crack throughout the corrosion region and some vertical cracks on side face before loading .It was observed that first vertical crack appeared at a load of 15.5 KN near the centre of beam on side face, with widening of longitudinal crack at the centre and as the load on beam was increased, vertical crack from tension zone propagates towards the compression face till the longitudinal crack and finally beam fails at a load of 21.3 KN with a huge crack at centre of beam.

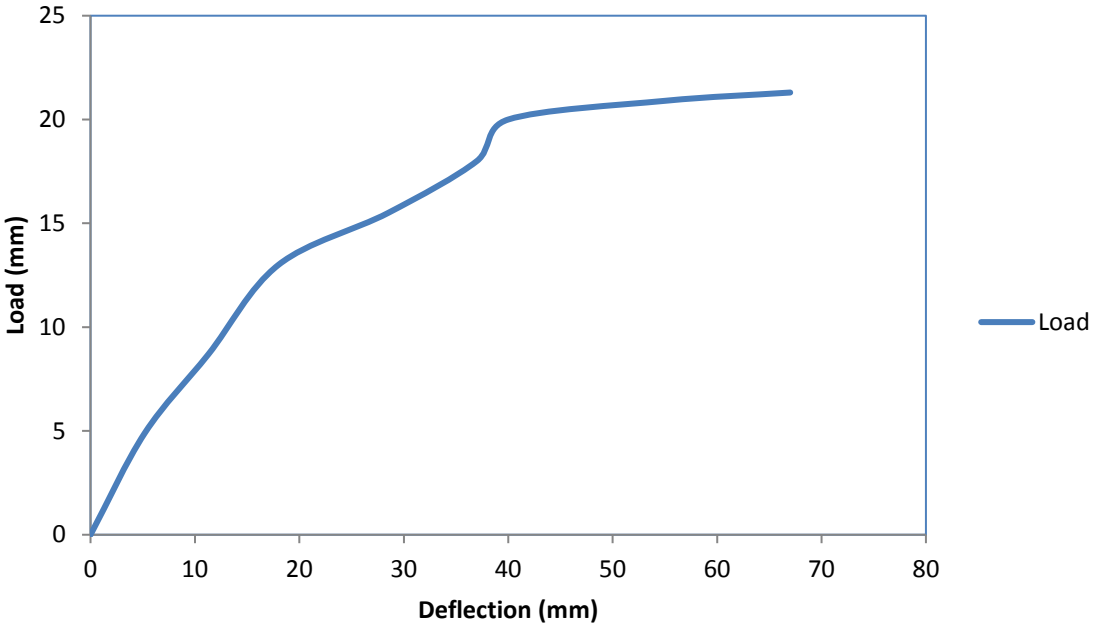

Figure 4.18 Load deflection curve of beam C-30 At L/2

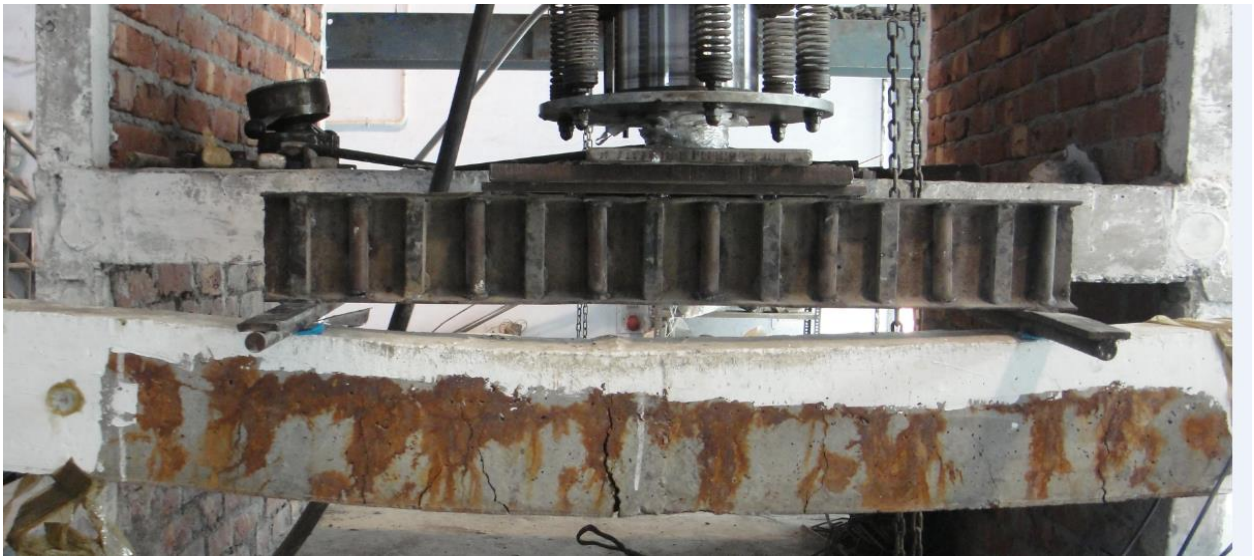

Figure 4.19 C-30 Beam showing large vertical crack near the centre of beam

4.3.4 Beams corroded to 40 days (C-40)

Beam undergoing corrosion for 40 days shows longitudinal crack throughout the corrosion region and some vertical cracks on side face before loading .It was observed that first vertical crack appeared at a load of 12 KN near the centre of beam on side face, with widening of longitudinal crack at the L/4 distance frome centre and as the load on beam was increased, vertical crack from tension zone propagates towards the compression face till the longitudinal crack and finally beam fails at a load of 20 KN with a huge crack at centre of beam.

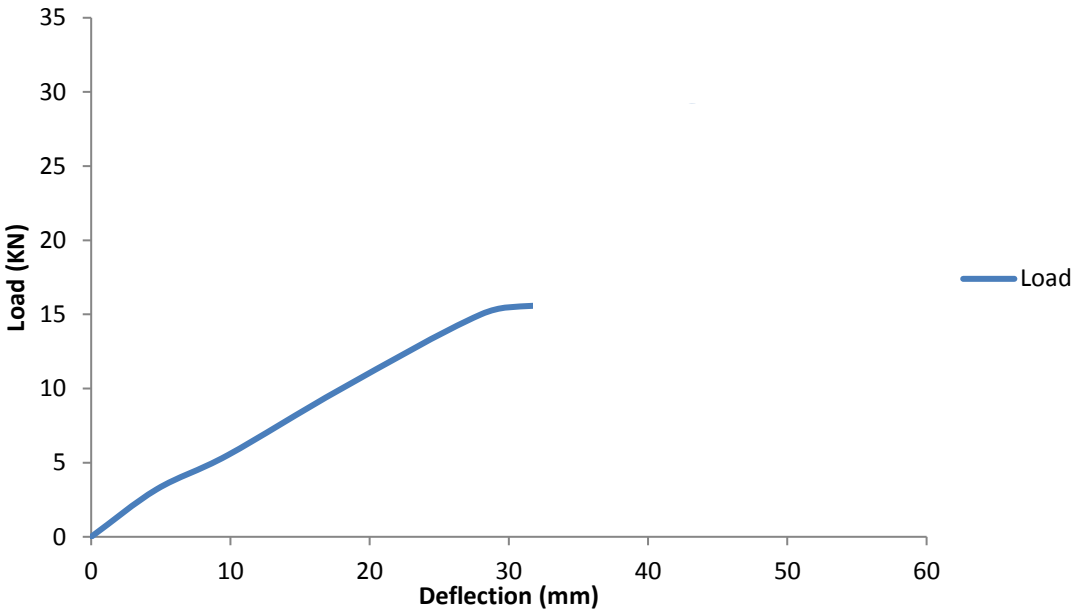

Figure 4.20 Load deflection curve of beam C-40 At L/2

Figure 4.21 C-40 Beam showing large vertical crack

4.3.5 Comparison of P - Δ characteristics of all beam

After studying **P -** Δ behaviour of all beams corroded to different extents, it can be concluded that load carrying capacity, deflection and stiffness degrades with progressive corrosion it also shows how the ductility in the beams reduces when corrosion increases indicated by reduction in load at first crack when corrosion increases. **Table 4.2** gives the stiffness loss in beams under increasing corrosion. As the corrosion level increases we can correlate with the visual inspection that cracks increases in beams leads to decrease in load carrying capacity of beams and hence stiffness decreases**. Figure 4.22** shows the graphical representation that how stiffness lost when corrosion level in beams increases

Table 4.2 Stiffness loss

Nomenclature	Ultimate load (KN)	Deflection L/2 (mm)	Stiffness (KN/mm)	Stiffness loss (%)	Load at first crack
C-0	27.87	82.03	0.32	0	22.5
C-20	25	79	0.316	1.25	18
C-30	21.3	71	0.3	6.25	15.5
C-40	20	67	0.29	9.37	12
C-60	-	-	-	-	-
F-60	15	52	0.28	12.5	-

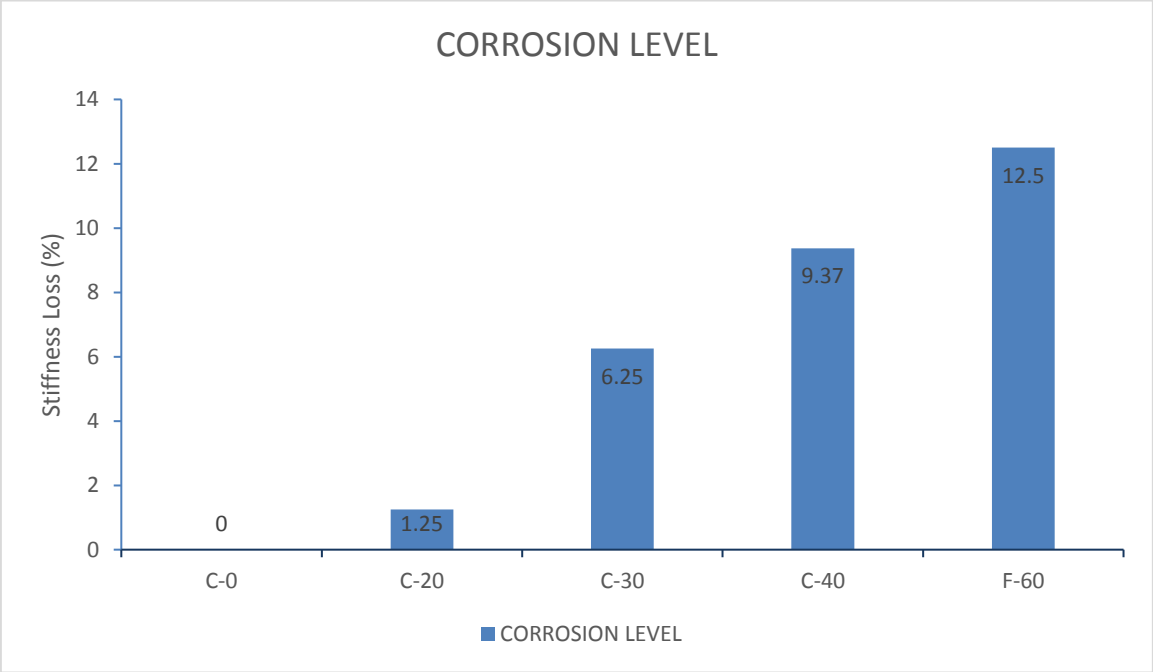

Figure 4.22 Bar chart showing stiffness loss with corrosion in beam

4.4 Acoustic Emission Testing Results :

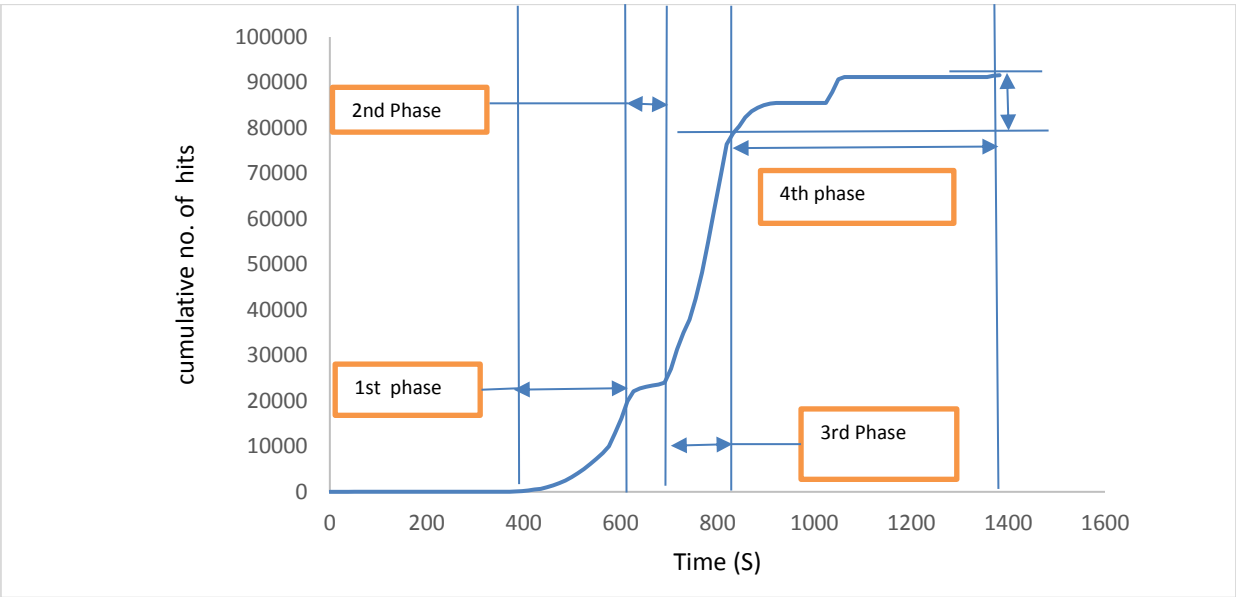

Figure 4.23 Cumulative AE hits Vs time (C-0)

4.4.1 AE record in healthy beam

In **Figure 4.23** the cumulative hits versus time as well as load versus time are plotted for the healthy specimen tested under flexural loading. The rate of increase of AE hits gives the characteristic of a material. Increasing the load was accompanied by the increased AE activity right from the start. The total no. of recorded hits lie between 9000-10000. The entire AE hit plot could be divided into four phases 1, 2, 3 & 4.

- During the phase 1, the AE hits increase gradually with the increase in load. This increase could be related with the development of micro cracks in concrete during the initial stages.
- After the phase 1, there is calm phase which is recorded and identified as Phase 2.During this phase the rate of increase of AE activity has decreased to a great extent. This could be well related with the transition phase where the micro cracks are being converted into the macro cracks.

- The 3rd phase which observed a steep rise in the number of recorded hits reveals the formation of macro cracks. It was also observed that during the phase 3, the cracks also started appearing on the surface of the beam.
- During the 4th phase, the number of AE hits recorded was very low and this could be due to the attenuation of AE signal with the development of major cracks.

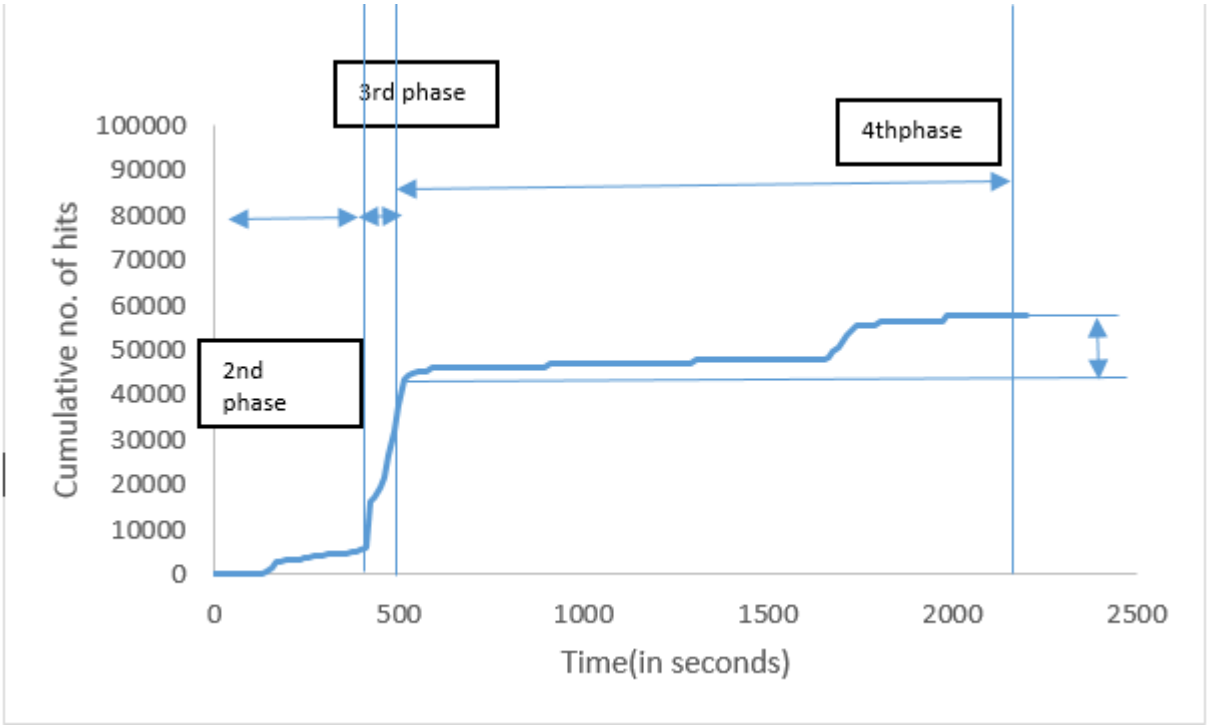

Figure 4.24 AE monitoring of C20 specimen

4.4.2 AE record of C-20

The results from AE monitoring of C20 specimen are shown in the **Figure 4.24**. The specimen was corroded for a period of 20 days continuously using accelerated corrosion technique. From the flexural test under two point loading, it can clearly be seen that the phase 1 as observed in the case of the healthy beam was completely missing. This very well correlates with the fact that the micro-cracking had already taken place due to corrosion and hence was not observed. All other phases 2, 3 &4 was clearly observed in the AE hit plot. 3 number of hits that were recorded were very less in comparison to that of healthy beam which also points towards the missing phase 1 from the graph.

- The micro cracks coalesce further in 2nd and 3rd phase to become macro- cracks
- It indicates that in an already cracked beam due to corrosion the initiation of cracking denoted by phase 1 by amplitude and large number of cracks is missing as the beam is already corroded and cracked.
- The cracking further due to loading is picked by AE sensors in phase 2,3 and 4.

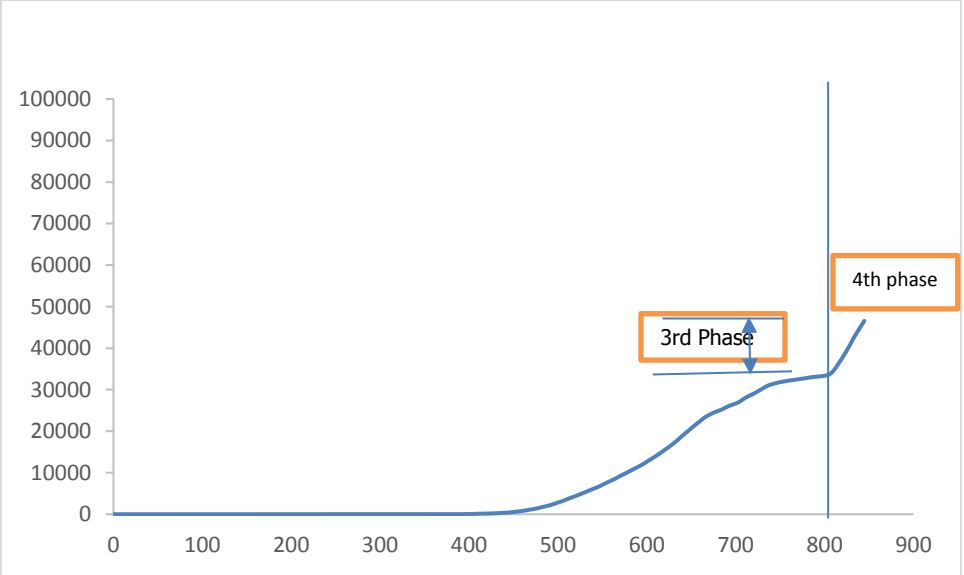

Figure 4.25 AE monitoring of C30 specimen

4.4.3 AE Record of C–30

The **Figure 4.25** represents the results from AE monitoring of C30 specimen. The specimen was corroded upto a period of 30 days was subjected to AE monitoring while loading. Following observation are obtained:

- The behaviour of AE hit plot in this case clearly shows the absence of first two phases i.e. phase 1 and phase 2.
- The number of AE hits that are recorded are also lesser than it was recorded for C-0 and C-20.

4.4.4 AE Record of C-40

And in the **Figure 4.26**, the results from AE monitoring of C40 specimen are plotted. The specimen was corroded for a period of 40 days SIGNIFICANT OBSERVATION:

- Only phase 4 is observable in this plot. This signifies that both the minor and major cracking had already occurred due to the corrosion of reinforcement.
- Only small cracking leading to total failure of the structure was observed.
- It can also be observed that the number of AE hits recorded during the phase 4 are almost same in all the cases.

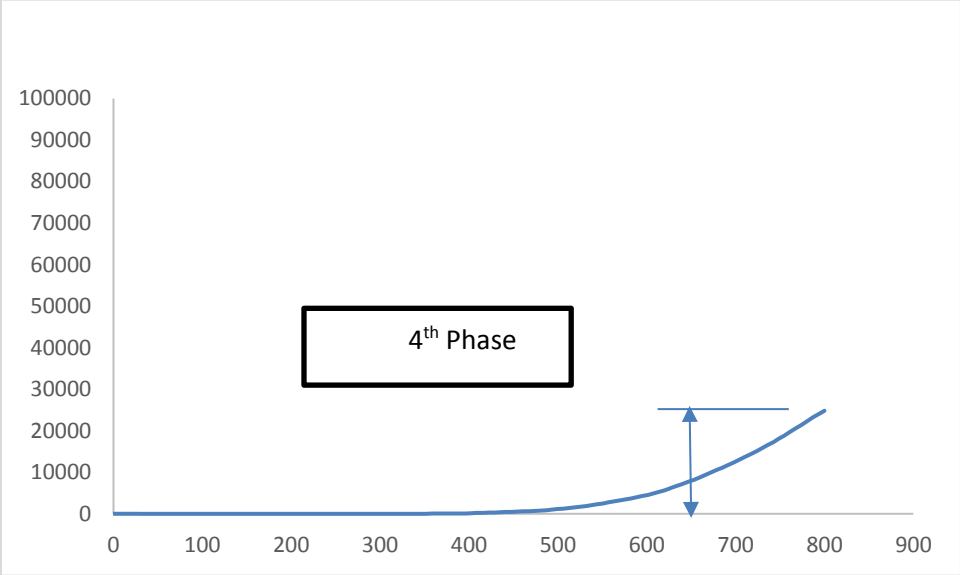

Figure 4.26 AE monitoring of C40 specimen

Therefore, following points can be drawn from the destructive testing using AE technique while subjected to flexural loading:

1) AE hits very clearly characterize the whole cracking process under flexural loading into four phases: Phase 1, 2, 3& 4. Phase 1 and 3, correspond to the micro- and macro-cracking respectively.
2) AE technique can effectively bring out the variations in the cracking behaviour of RC specimen when corroded beams are subjected to flexural loading.

3) AE is less effective after macro cracking has occurred because of the attenuation of signal due to larger cracks as could be seen in phase 4. Wherein, the no. of hits recorded are very less.
4) Different stages of cracking phenomena in corroded beams when subjected to loading can be easily assessed from AE .

Hence AE technique along with P- Δ curves give a good indication of cracking pattern of corroded beams along with P- Δ characteristics of first crack formation, stiffness loss and it correlates well with the degree of deterioration of beam due to corrosion.

4.4.5 Closing Remarks

Highlights the results obtained from the experiments done during the thesis work. It shows results of visual observations of RC beams subjected to different levels of corrosion and its effect on load deflection behaviour when the RC beams were tested under static two point loading. From the results it was observed that there is decrease in ultimate load, deflection capacity, stiffness as the corrosion level increases. This section also deals with the results of FRF recorded during vibration monitoring of RC beam which shows the effect of corrosion on dynamic properties of beams like natural frequency and FRF amplitude and AE hit parameters which characterize the whole cracking process under flexural loading into four phases: Phase 1, 2, 3& 4. Phase 1 and 3, correspond to the micro- and macro-cracking respectively.

4.5 C-60 Beam Retrofitted with GFRP (F-60)

4.5.1 P - Δ Behaviour of F-60

Beam undergoing corrosion for 60 days shows longitudinal crack throughout the corrosion region and some vertical cracks on side face so it was retrofitted with GFRP**.** It was observed that first vertical crack appeared at a load of 11.2 KN near the center of beam on side face, with widening of longitudinal crack at the center **Figure 4.28** and as the load on beam was increased and finally beam fails at a load of 17.6 KN with a huge crack at center of beam as shown in **Figure 4.27**.

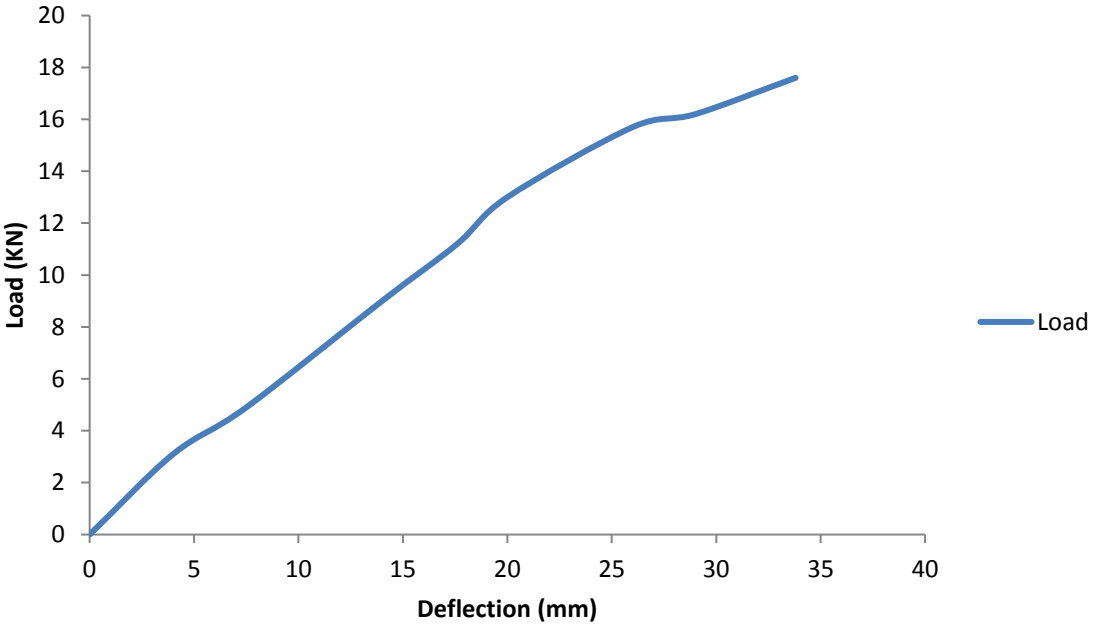

Figure 4.27 Load deflection curve of beam F-60 At L/2

Figure 4.28 F-60 Beam cracked from the centre

4.5.2 AE Record for F-60 specimens:

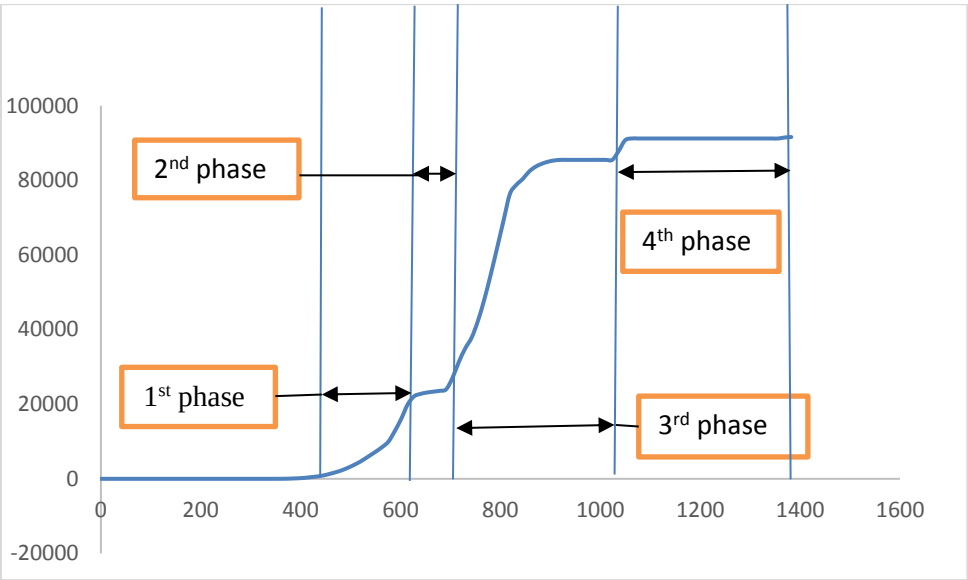

Figure 4.29 AE Record of F-60

Figure 4.29 shows the plot of C-60 specimen wrapped using GFRP and monitored under flexure using AE technique. The recorded no. of hits for this specimen and the healthy specimen is somewhat close. This implies that the GFRP has successfully strengthened the corroded beam. Secondly, the rate of increase of AE hit is also similar to that of the healthy beam and all four phases are easily identifiable. This further suggest the beam corroded for 60 days and then wrapped with GFRP would behave like the healthy beam under the Flexural loading. Therefore, it can be said that GFRP wrap for reinforcing the RC beam would surely improve the Flexural behavriou of the beam to a great extent.

CHAPTER 5

Conclusions and recommendations

5.1 VISUAL INSPECTION

From the reinforced concrete beams subjected to accelerated corrosion at different levels i.e.20 days, 30 days, 40days, 50 days and 60 days all beams were visually inspected and it was observed that as exposure time of the beams to corrosion increases deterioration increases. Following results are observed:

- For C-20 That's 20 days specimen at a constant voltage of 10V shows only reddish brown corrosion patches on the centre 1.5 m portion of beam which was intentionally corroded . No cracks were developed on the surface of the beam
- For C-30 That's 30 days specimen at a constant voltage of 10V shows small horizontal and vertical cracks on the surface of beam of increased length and width and increase in volume of corrosion product was noticed.
- For C-40 That's 40 days specimen at a constant voltage of 10V shows comparatively large horizontal and vertical cracks on the surface of beam of increased length and width and increase in volume of corrosion product was noticed
- For C-50 That's 50 days specimen at a constant voltage of 10V shows large vertical cracks in the centre of beam along with horizontal and vertical on the surface of beam ere noticed with increase in of corrosion.
- For C-60 That's 60 days specimen at a constant voltage of 10V show beams, it was observed that the cracks has covered full longitudinal length at middle 1.5m portion of RC beam and corrosion products generated were of dark and Flexural crack also observed at centre of beam.

This reddish brown product is a results of rusting of reinforcement in the beams and crack generation is because of tensile stresses generated due to increased volume of bar at cathode area, as we all know concrete is weak in tension so it results in cracking.concrete spalling is also observed during corrosion process.

5.2 Vibration analysis

Vibration analysis of beams was conducted using OROS software which gives us the FRF response of beams including maximum amplitude and frequency of control beam and corroded beams.

- As the level of corrosion increases from control beam to 20days, 30days and 40days amplitude of vibrations goes on decreasing due to increased amount of deterioration
- Natural frequency of beam also decreases from 18.5Hz to 16 Hz with increasing level of corrosion.
- With increasing damage index amplitude of vibrations decreases.

As observed by visual inspection , with increases in corrosion level, cracks developed in beams which effects the static as well as dynamic properties of beams. As the level of corrosion increases, load at failure reduces pointing towards stiffness loss with increase in corrosion . In the same manner there is a huge decrease in FRF amplitude and natural frequency due to increased deterioration of beams .

5.3 Load deflection

Beams were subjected to static two point loading and load deflection curves reveal much information about the behaviour of beams. Static load tests showed the following results

- Ultimate deflection of corroded beams decreases s compared to control beam. The corrosion level increases , deflection at initial stages increases.
- A higher corrosion level results in decrease in stiffness.
- As the corrosion increases there is decrease in stiffness , load carrying capacity, deflection capacity thus it suggests a change in behaviour of beams from ductile to brittle.

5.4 AE analysis

- The AE hits very clearly characterize the whole cracking process under flexural loading.
- The AE technique can effectively bring out the variations in the cracking behaviour of RC specimen subjected to different degrees of damage due to corrosion.
- AE is less effective after macro cracking has occurred because of the attenuation of signal due to larger cracks as could be seen in phase 4. Wherein, the no. of hits recorded are very less.
- Different levels of deterioration in RC specimens could be distinguished using the AE hit parameter.

REFERENCES

1. Ahmad, S., & Shabir, Z. (2005). Effect of Water Cement ratio on Corrosion of Reinforced concrete. In *30th Conference on Our World In Concrete And Structures*.
2. El Maaddawy, T., Soudki, K., & Topper, T. (2005). Long-term performance of corrosion damaged reinforced concrete beams. *ACI Structural Journal*, *102*(5), 649.
3. https://scholar.google.co.in/scholar?hl=en&q=CORROSION+MECHANISM&btnG
4. Saraswathy, V., & Song, H. W. (2005). Performance of galvanized and stainless steel rebars in concrete under macrocell corrosion conditions. *Materials and Corrosion*, *56*(10), 685-691.
5. Song, H. W., & Saraswathy, V. (2007). Corrosion monitoring of reinforced concrete structures-a. *Int. J. Electrochem. Sci*, *2*, 1-28.
6. Da Fonseca, B. S., Castela, A. S., Ferreira, M. G. S., Duarte, R. G., Silva, M. A. G., & Montemor, M. F. Assessment of the effect of GFRP on the corrosion of steel reinforcement in confined RC by EIS.
7. https://www.google.co.in/search?espv=2&rlz=1C1CHWA_enIN649IN649&biw=1536&bih=737&tbm=isch&sa=1&q=GFRP+&oq=GFRP+&gs_l=img.3.
8. https://www.google.co.in/search?q=cfrp&espv=2
9. Baghiee, N., Esfahani, M. R., & Moslem, K. (2009). Studies on damage and FRP strengthening of reinforced concrete beams by vibration monitoring. *Engineering Structures*, *31*(4), 875-893.
10. Salawu, O. S. (1997). Detection of structural damage through changes in frequency: a review. *Engineering structures*, *19*(9), 718-723.
11. Mirmiran, A., & Philip, S. (2000). Comparison of acoustic emission activity in steelreinforced and FRP-reinforced concrete beams. *Construction and Building Materials*, *14*(6), 299-310.

12. Burgueño, R., Karbhari, V. M., Seible, F., & Kolozs, R. T. (2001). Experimental dynamic characterization of an FRP composite bridge superstructure assembly. *Composite Structures*, *54*(4), 427-444.

13. Maia, N. M. M., Silva, J. M. M., Almas, E. A. M., & Sampaio, R. P. C. (2003). Damage detection in structures: from mode shape to frequency response function methods. *Mechanical Systems and Signal Processing*, *17*(3), 489-498.

14. Kao, C. Y., & Hung, S. L. (2003). Detection of structural damage via free vibration responses generated by approximating artificial neural networks. *Computers and Structures*, *81*(28), 2631-2644.

15. Fan, W., & Qiao, P. (2011). Vibration-based damage identification methods: a review and comparative study. *Structural Health Monitoring*, *10*(1), 83-111.

16. Capozucca, R. (2013). A reflection on the application of vibration tests for the assessment of cracking in PRC/RC beams. *Engineering Structures*, *48*, 508-518.

17. Ohno, K., & Ohtsu, M. (2010). Crack classification in concrete based on acoustic emission. *Construction and Building Materials*, *24*(12), 2339-2346.

18. Behnia, A., Chai, H. K., Yorikawa, M., Momoki, S., Terazawa, M., & Shiotani, T. (2014). Integrated non-destructive assessment of concrete structures under flexure by acoustic emission and travel time tomography. *Construction and Building Materials*, *67*, 202-215.

19. Ono, K. (2011). Application of acoustic emission for structure diagnosis. *Diagnostyka*-Diagnostics and Structural Health Monitoring 2(58).

20. Xu, J. G. (2008). Nondestructive evaluation of prestressed concrete structures by means of acoustic emissions monitoring.

21. Yoon, D. J., Weiss, W., & Shah, S. (2000). Detecting the extent of corrosion with acoustic emission. *Transportation Research Record: Journal of the Transportation Research Board*, (1698), 54-60.

22. Colombo, S., Forde, M. C., Main, I. G., & Shigeishi, M. (2005). Predicting the ultimate bending capacity of concrete beams from the "relaxation ratio" analysis of AE signals. *Construction and Building Materials*, *19*(10), 746-754.

23. Yun, H. D., Choi, W. C., & Seo, S. Y. (2010). Acoustic emission activities and damage evaluation of reinforced concrete beams strengthened with CFRP sheets. *NDT & E International*, *43*(7), 615-628.

24. Ohno, K., & Ohtsu, M. (2010). Crack classification in concrete based on acoustic emission. *Construction and Building Materials*, *24*(12), 2339-2346.

25. Antonaci, P., Bocca, P., & Masera, D. (2012). Fatigue crack propagation monitoring by Acoustic Emission signal analysis. *Engineering Fracture Mechanics*, *81*, 26-32.

26. Aldahdooh, M. A. A., & Bunnori, N. M. (2013). Crack classification in reinforced concrete beams with varying thicknesses by mean of acoustic emission signal features. *Construction and Building Materials*, *45*, 282-288.

27. Nor, N. M., Ibrahim, A., Bunnori, N. M., & Saman, H. M. (2013). Acoustic emission signal for fatigue crack classification on reinforced concrete beam. *Construction and Building Materials*, *49*, 583-590.

28. Gadve, S., Mukherjee, A., & Malhotra, S. N. (2011). Active protection of fiber-reinforced polymer-wrapped reinforced concrete structures against corrosion. *Corrosion*, *67*(2), 1-11.

29. Kanwar, V., Kwatra, N., Aggarwal, P., & Gambir, M. L. (2006). Vibration monitoring of a RCC building model. In *Proceedings of National Conference on Technology for Disaster Mitigation*, 277-285.

ORIGINALITY REPORT

15%	7 %	15%	8%
SIMILARITY INDEX	INTERNET SOURCES	PUBLICATIONS	STUDENT PAPERS

PRIMARY SOURCES

1	Sharma, Ashutosh, Shruti Sharma, Sandeep Sharma, and Abhijit Mukherjee. "Ultrasonic guided waves for monitoring corrosion of FRP wrapped concrete structures", Construction and Building Materials, 2015. Publication	1%
2	Gadve, Sangeeta Mukherjee, A. Malhotra, . "Corrosion of steel reinforcements embedded in FRP wrapped concrete.(Statistical table)", Construction and Building Materials, Jan 2009 Issue Publication	1%